Energy management of a hybrid locomotive equipped with fuel cell, batteries, supercapacitors and intermittent access to the electrical network

Diana Sofía Mendoza Contreras

Submitted in partial fulfillment of the requirements for the degree of Master in Electrical Engineering

Director

Javier Solano Martínez

PhD Electrical Engineering

Codirector

Loïc Boulon

PhD Electrical Engineering

Universidad Industrial de Santander

Facultad de Ingenierías Fisicomecánicas

Escuela de Ingenierías Eléctrica, Electrónica y de Telecomunicaciones

Bucaramanga

2021

Table of Contest

List of Figures

List of Tables

List of Appendix

Page

Resumen

Título: Gestión de energía de una locomotora híbrida dual equipada con pila de combustible, baterías, supercondensadores y acceso intermitente a la red eléctrica [*]

Autor: Diana Sofía Mendoza [**]

Palabras Clave: Gestión de energía, vehículo híbrido, batería, locomotora dual, supercondensador, pila de combustible, repartición de potencia.

Descripción: Este trabajo de investigación de maestría propone una estrategia de gestión de energía (EMS por sus siglas en inglés) para una locomotora híbrida de modo dual equipada con pila de combustible, supercondensadores y baterías, y acceso intermitente a una catenaria aérea electrificada. La EMS modular define la distribución de energía entre las fuentes de energía respetando las restricciones en las variables eléctricas del sistema. La estrategia está inspirada en el diagrama de Ragone, el cual relaciona las características de potencia y energía de cada una de las fuentes. La EMS no considera información o predicciones del consumo de carga futuro. La EMS en tiempo real propuesta tiene como objetivo reducir una función de costo que considera el costo del hidrógeno, la electricidad consumida de la red y la degradación de las fuentes de energía. Esta estrategia propuesta se centra en maximizar la energía recuperada durante el frenado. El trabajo de investigación también introduce una metodología original para ajustar los valores del conjunto de parámetros de la EMS, la cual se basa en el método experimental. Se emplean dos casos de estudio para evaluar la EMS propuesta. Los resultados muestran que existe una oportunidad real de aumentar la energía recuperada durante el frenado si se realiza una EMS apropiada.

---

[*] Trabajo de investigación

[**] Escuela de Ingenierías Eléctrica, Electrónica y telecomunicaciones. Director: Javier Solano Martínez, PhD. Ingeniería Eléctrica

Abstract

Title: Energy management of a hybrid locomotive equipped with fuel cell, batteries, supercapacitors and intermittent access to electric network [*]

Author: Diana Sofía Mendoza [**]

Keywords: Energy management, hybrid vehicle, battery, dual-mode locomotive, supercapacitors, split power, fuel cell.

Description: This master thesis proposes an energy management strategy (EMS) for a dual-mode hybrid locomotive equipped with a fuel cell, supercapacitors and batteries, and intermittent access to an electrified overhead catenary. The modular EMS defines the power distribution between the power sources respecting constraints in the electrical variables. It is inspired by the Ragone-plot and doesn't consider information or predictions of the future load consumption. The proposed real-time EMS aims to reduce a cost function that considers the cost of the hydrogen, the electricity consumed from the network and the degradation of the energy sources. The EMS focuses on maximising the energy recovered during braking. The research work also introduces an original methodology to tune the values for the set of parameters of the EMS. Two study-cases are used to evaluate the proposed EMS. The results show that there is a real opportunity to increase the energy recovered during braking if a proper EMS is performed.

---

[*] Research Work

[**] Escuela de Ingenierías Eléctrica, Electrónica y telecomunicaciones. Director: Javier Solano Martínez, PhD Electrical Engineering.

Introduction

A dual-mode locomotive has a common drivetrain that operates on not- and electrified tracks. It allows driving a locomotive in a partially electrified railway. Considering the high cost of the network electrification, this is a good compromise to reduce energy consumption in rail transport Lhomme et al. (2018a). In this regard, Fuel cell (FC) locomotives are considered as a great alternative to moving away from locomotives using diesel engines Din and Hillmansen (2018); Hoffrichter et al. (2016); Hong et al. (2018); Li et al. (2017); Sarma and Ganguly (2019); Yoneyama et al. (2007); Yedavalli et al. (2011). FC are not reversible and the responsiveness of the gas supply limits its response. Therefore, the time constants as obtained from step responses of electrical power are rather, pointing to a rather low bandwidth and a low access speed Strunz and Brock (2006). For these reasons, the FC cannot be considered as a unique source for electrical locomotives. Supercapacitors (SC) and batteries offer a high efficiency and a high speed of access to electrical energy. They are therefore, an ideal complement to the fuel cell in hybrid electric locomotives Baert et al. (2013); Jaafar et al. (2009); Strunz and Louie (2009); Radu et al. (2019).

Control of FC, and in general, hybrid locomotives is a very complex problem. For the sake of ease, it can be subdivided into two independent problems: to define driving strategies based on optimal speed trajectories and to determine power distribution among the available sources.

Many researches aim to define optimal speed trajectories using analytical techniques such

as Pontryagin Minimum Principle Khmelnitsky (2000); Albrecht et al. (2016); Liu and Golovitcher (2003) or numerical methods such as dynamic programming Franke et al. (2000); Sorrentino et al. (2020); Haahr et al. (2017). These techniques require a perfect knowledge of the operating conditions during a mission. This could be true for a great number of locomotives periodically running on the same track according to a strict timetable.

Methodologies to determine optimal train speed profiles are proposed in both theory and applications, but they are complicated and complex to achieve. In real operation conditions, the train may not always follow the planned schedule. It wont arrive at or depart from the station on time because of unpredictable traffic conditions, unplanned stops, unsteady driving behaviors, passenger demand variations, infrastructure failures, or even the willingness of the train driver to follow the recommended speed profile Yin et al. (2016); Lanneluc et al. (2018); Yang et al. (2018).

As these optimal speed profiles are theoretical but difficult to follow, then real-time operation adjustment recommended Gu et al. (2014). Therefore, developing on-line algorithms that consider dynamic situations such as traffic in the path ahead may be more applicable for practical purposes Saadat et al. (2016). Heuristic solutions such as Fuzzy logic Cucala et al. (2012); Saadat et al. (2016) or genetic algorithms Bocharnikov et al. (2007); Hwang (1998) are often proposed to define the optimal speed trajectory references.

Once the speed profile is determined, using the dynamical model of the train, braking and

traction forces profiles are computed. These are used to compute power profiles in the locomotive power bus. The new challenge consists of defining the power and energy distribution among the available sources. Energy management strategies (EMS) are designed to determine power and energy distributions among the energy sources for a given bus power profile. The solutions aim to minimize a multi-objective cost function while respecting static and dynamic constraints to limit the power, currents and the state-of-charge (SOC) of the energy storage sources.

As stated before, in real operation conditions, it is not easy to predict power profiles, and then real-time EMS are more than desirable. The proposed EMS should guarantee good performances even without knowledge of train speed and power profiles. Rule-based approaches lean on human experience to design EMS algorithms to define the power distribution. Compared with other approaches, these strategies are intuitive and easier to implement. Many researches propose rule-based methodologies to determine the power distribution in hybrid trains Allègre et al. (2010); Ciccarelli et al. (2012); Iannuzzi and Tricoli (2012); Radu et al. (2019).

The energy dissipated during train braking particularly in suburban, rural and freight trains can be very high. In some cases, as the urban systems the energy can be recovery trough the catenary. In some urban rail systems, this value can be up to 50 % of the net traction energy González-Gil et al. (2014, 2013). Thus, it is not surprising that one of the most significant opportunities to reduce the energy consumption in trains is to perform an efficient use of energy regenerated during braking. Regenerative braking can be used by other trains, but it is only possible if, at the same

time, a train is accelerating and another is braking, then a sophisticated, coordinated train control and time-scheduling is required Gordon and Lehrer (1998); Kampeerawat and Koseki (2019); Khayyam et al. (2018). These approaches are promising at least in theory, however in real operation, they are still very complex to implement. The braking energy can be supplied to the power system using substations that require a very high investment at least in DC networks González-Gil et al. (2013).

Embedded energy storage sources such as supercapacitors or batteries are used to perform recovery braking. They are a more viable alternative to recover energy during braking. This option is similar to the one used in application with a high start/stop frequency such as elevators driven by synchronous machines Raghavendra Rao and Mahesh (2018); Rao et al. (2018). These embedded sources present additional advantages such as reduction of peak power demand, reduction of energy losses in the catenary and a certain degree of autonomy for catenary-free services González-Gil et al. (2014).

Most of the works published in energy recovering using embedded sources focus on metro trains and tramways, considering their frequent start/stops. Most of these researches estimates a reduction in total energy consumption around 12-35 % when using SC. Simulation results reported in literature shows reductions of 33 % for a metro line in Brussels Barrero et al. (2008), 24 % for a metro line in Madrid Domínguez et al. (2011), 25 % for a tramway in Mannheim Destraz et al. (2007), or 30 % for and 30 % for a Blackpool tramway Chymera et al. (2008) are reported in litera-

ture. The research presented in Lanneluc et al. (2018), oriented to freight trains, shows that using a storage unit to enable regenerative braking reduces up to 25 % of the total energy.

Experimental research has pointed out that supercapacitors can recover most of the energy recovered in braking Solano et al. (2013); Ciccarelli et al. (2012); Iannuzzi and Tricoli (2012). An experimental study suggests a reduction around 16 % energy savings in a tramway in Paris Moskowitz and Cohuau (2010). Moreover, experimental tests performed so far on a light railway vehicle prototype of Bombardier Transportation have highlighted that the energy saved using SCs could be approximately equal to 30 % Steiner et al. (2007).

This work aims to solve the problem proposed in the IEEE VTS motor vehicles challenge 2019 - energy management of a dual-mode locomotive Lhomme et al. (2018b). It consists in proposing an EMS for a dual-mode locomotive equipped with a fuel cell, supercapacitors, batteries and access to an electrified overhead catenary. The solution must minimize a cost function that considers the consumption of the electricity network, the consumption of the hydrogen, the lifetime of the fuel cell and the lifetime of the energy sources. The solutions to the challenge must respect an additional constraint: no previous knowledge of the speed or power profile is allowed to compute the power distribution.

This work proposes an extended version of the research presented in Mendoza et al. (2019), which was the best solution submitted to the IEEE VTS motor vehicles challenge 2019. This EMS

has new objectives such as maximizing the energy recovered during braking, which can represent an important part of the total energy losses of the train. The report is organized as follows: Section 2 introduces the global energy management strategy. Then it presents the local energy management strategies for the fuel cell, batteries, supercapacitors and DC bus capacitor. Section 3 presents simulation results, and Section 4 presents the conclusions.

1. Objectives

1.1. General Objective

Design, implement and evaluate a power flow distribution strategy that reduces the overall operating cost of a dual locomotive.

1.2. Specific objectives

Design a rule-based energy management strategy for a dual-mode locomotive equipped with batteries, fuel cells, supercapacitors and access to the electrical network, presented inLhomme et al. (2018a).

Implement the proposed strategy in MATLAB-Simulink.

Evaluate the proposed strategy by comparing it with the strategy presented in Mendoza et al. (2019). The proposed strategy should reduce the global cost function defined in Lhomme et al. (2018a), which considers the degradation of sources, hydrogen consumption and the change in the state of charge in energy storage systems.

2. Model of the dual-mode locomotive

The considered hybrid locomotive can be powered by a non-reversible DC overhead line through a pantograph or using an on-board fuel cell (FC) with batteries and supercapacitors (SC). The sources are connected to the DC bus using power converters. The characteristics of locomotive sources and power converters are presented in Appendix 2. Figure 1 presents the schematic of the dual-mode locomotive.

Figure 1. Structural scheme of the studied locomotive

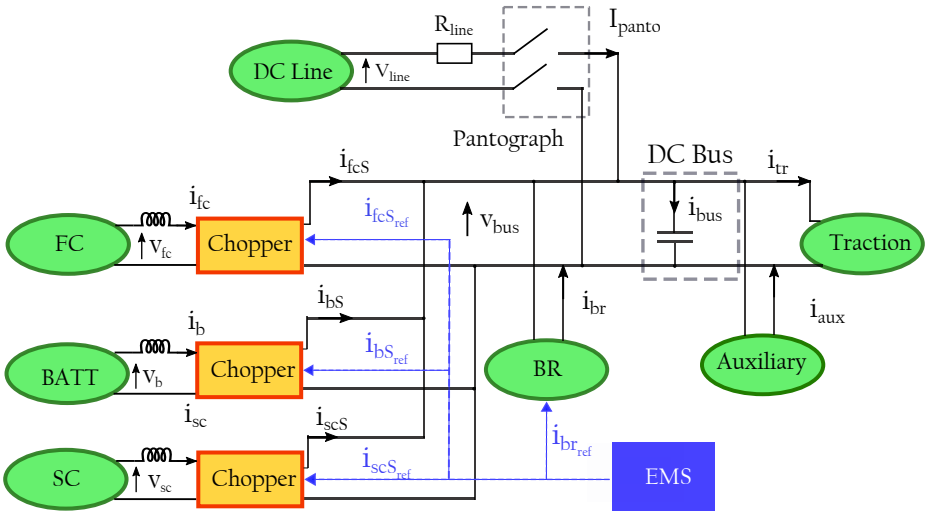

The proposed Energy Management Strategy (EMS) defines current references for the fuel cell system $i_{fcS}(t)$, the battery system $i_{bS}(t)$, the supercapacitor system $i_{scS}(t)$ and the braking resistor $i_{br}(t)$. The current supplied by the pantograph $i_{pant}(t)$, when available, and the current supplied to/by the DC bus capacitor i_{bus} depend on the DC bus capacitor voltage which can be indirectly controlled. The current consumed by the motor drives $i_{tr}(t)$ and the ancillary $i_{aux}(t)$ are not known a priori. The current distribution between the sources and loads, at the DC bus level,

respects the balance defined in Equation 1.

$$i_{fcS}(t) + i_{bS}(t) + i_{scS}(t) + i_{br}(t) + i_{pant}(t) = i_{tr}(t) + i_{aux}(t) + i_{bus}(t) \quad (1)$$

2.1. Constraints

The solutions must respect constraints in the sources powers, currents, voltages and SOC. One additional challenge to consider, is that the EMS references are given at the DC bus level, after the power converters, but most of the constraints are given in the terminals of each source before the power converters.These constraints are defined for the voltage and current in the terminals of the fuel cell $i_{fc}(t)$, $v_{fc}(t)$, the battery $i_b(t)$, $v_b(t)$ and the supercapacitor $i_{sc}(t)$, $v_{sc}(t)$. The batteries and supercapacitors states-of-charge SOC SOC_b, SOC_{sc} are also constrained. Additional constraints are given for the power supplied by the power converters $p_{scS}(t)$, $p_{fcS}(t)$, $p_{bS}(t)$ and $p_{br}(t)$.

The restrictions for a generic source k and its power converter ks are presented below.

$$V_{\mathrm{kmin}} < v_{\mathrm{k}}(t) < V_{\mathrm{kmax}} \quad (2)$$

$$SOC_{\mathrm{kmin}} < SOC_{\mathrm{k}}(t) < SOC_{\mathrm{kmax}} \quad (3)$$

$$I_{\mathrm{kmin}} < i_{\mathrm{k}}(t) < I_{\mathrm{kmax}} \tag{4}$$

$$\frac{dI_{\mathrm{k}}}{dt}_{\min} < \frac{di_{\mathrm{k}}}{dt}(t) < \frac{di_{\mathrm{k}}}{dt}_{\max} \tag{5}$$

$$P_{\mathrm{ksmin}} < p_{\mathrm{ks}}(t) < P_{\mathrm{ksmax}} \tag{6}$$

2.2. Cost function

The viable solutions are evaluated and compared using a multi-objective function $€_{tot}$ composed of six cost functions to minimize Lhomme et al. (2018a):

1. the hydrogen consumption $€_{H_2}$. It depends on the H_2 mass flow, which at its time depends on the current supplied by the fuel cell.

$$\varepsilon_{H_2}(t) = \frac{H_{2-\mathrm{cost}}}{1.10^3} \int_0^t \dot{m}_{H2}(t)dt \tag{7}$$

with $\dot{m}_{H2}(t)$ the hydrogen mass flow (g/s) and $H_{2-\mathrm{cost}}$ the hydrogen cost per unit of hydrogen mass (€/kg).

2. the FC degradation $€_{fc}$. The fuel cell degradation function $\Delta_{fc}(t)$ depends on the power operation $p_{fc}(t)$ and the start number N_{start} of the fuel cell.Chen et al. (2015); Herr et al.

(2017)

$$\Delta_{fc}(t) = N_{\text{start}}\Delta_{\text{start}}(t) + \int_0^t \delta(t)dt \tag{8}$$

$$\delta(t) = \frac{\delta_0}{3600}\left(1 + \frac{\alpha}{P_{fc-rat}^2}\left(p_{fc}(t) - P_{fc-rat}\right)^2\right) \tag{9}$$

with $\Delta_{\text{start}}(t)$ the start-stop degradation coefficient, δ_0 and α load coefficients and P_{fc-rat} the rated power of the fuel cell (W). The operational cost of the fuel cell can then be deduced from $\Delta_{fc}(t)$

$$\varepsilon_{fc}(t) = \frac{P_{fc-rat}}{1.10^3} FC_{cost}\Delta_{fc}(t) \tag{10}$$

with FC_{cost} the fuel cell cost per unit of power (€ /kW).

3. the SC degradation $€_{sc}$.

The degradation function of the supercapacitors $\Delta_{sc}(t)$ is calculated by the ratio between the use time t_{use} and the expected lifetime:

$$\Delta_{SC}(t) = \frac{t_{use}}{30.10^3} \tag{11}$$

The operational cost of the supercapacitors can then be deduced from $\Delta_{sc}(t)$

$$\varepsilon_{sc}(t) = E_{sc-rat} SC_{cost} \Delta_{sc}(t) \tag{12}$$

with E_{sc-rat} the rated energy of the supercapacitors (kWh) and SC_{cost} the supercapacitors cost per unit of energy (€/kWh)

4. the batteries degradation $€_{bat}$.

The battery degradation function $\Delta_b(t)$ depends of the state of charge with $f(\text{SOC}_b)$ and power dynamics with $g(i_b)$ *Babazadehet al.* (2014)

$$\Delta_b(t) = \frac{1}{3600.15 \cdot 10^3 \cdot Q_{b-rat}} \int_0^t |f(SOC_b) \cdot g(i_b) \cdot i_b(t)| \, dt \tag{13}$$

with $Q_{b-\text{rat}}$ and $i_b(t)$ respectively the rated capacity (Ah) and the current (A) of the battery.

The operational cost of the battery can then be calculated from $\Delta_b(t)$

$$\varepsilon_b(t) = E_{b-rat} B_{cost} \Delta_b(t) \tag{14}$$

with $E_{b-\text{rat}}$ the rated energy of the battery (kWh) and B_{cost} the battery cost per unit of energy (€/kWh).

5. the electricity consumed from the network $€_{net}$.

$$\varepsilon_{net}(t) = \frac{N_{cost}}{3600.1.10^6} \int_0^t p_{line}(t)dt \tag{15}$$

with $p_{\text{line}}(t)$ the instantaneous power (W) delivered by the DC line of the electricity network, and N_{cost} the cost of the electricity network per unit of energy (e/MWh), which takes into account the public electricity network tariffs.

6. the battery and SC charge sustaining cost after the cycle $€_{sust}$.

$$\varepsilon_{\text{sust}}(t) = \frac{N_{\text{cost}}}{1.10^3} \left(\eta_{dc-b-\text{avg}} \cdot E_{b-\text{end}} \quad + \eta_{dc-sc-\text{avg}} \cdot E_{\text{sc-end}} \right) \tag{16}$$

with $\eta_{dc-b-avg}$ and $\eta_{dc-sc-avg}$ the average value of the efficiency maps of the boost choppers; and E_{b-end} and E_{sc-end} the energy stored of the battery and supercapacitors at the end of the simulation (kWh). The sustainability cost $€_{sust}$ can be negative if the final SOC of the SC or batteries are higher than the initial.

3. Energy Management Strategy of a Dual-mode Locomotive

This chapter will present the proposed Energy Management Strategy for the dual-mode locomotive presented in Chapter 2. The Section 3.1 will present the strategy in a general way and the next sections will present the strategy in a particular way for each source of the system .

3.1. Global Energy Management Strategy

In the strategy, the fuel cell will delivery the average energy. The batteries and supercapacitors will assume the transient power, especially when there is a change in the required train power, the supercapacitors will delivery power at the first place. The supercapacitors must have an adequate SOC that allows them to recover energy during braking and delivery energy during acceleration. The batteries perform the SC SOC regulation. Each source has some particularities, and these will be explained bellow at the local strategies.

Considering the characteristics and constraints of each energy source, and inspired on the Ragone-plot illustrated in Figure 3, a rule-based global EMS is proposed and implemented. The Figure 2 presents the global EMS formed by local strategies for each source. The FC is the primary energy source embedded in the dual-mode locomotive. Together with the pantograph, when available, they must supply the total energy consumed by the traction system. However, during braking, the FC current is reduced to limit the energy dissipated in the braking resistor. The pantograph is an interesting source in terms of power and energy, but the EMS has to consider its intermittent availability (dual-mode EMS). The batteries are characterized by a good compromise between power and energy. They can be used to provide energy to the load and in regenerative braking. The SC, as the main power source of the locomotive, is used to balance the current in the Equation (1) .

Figure 2. Dual mode locomotive EMS

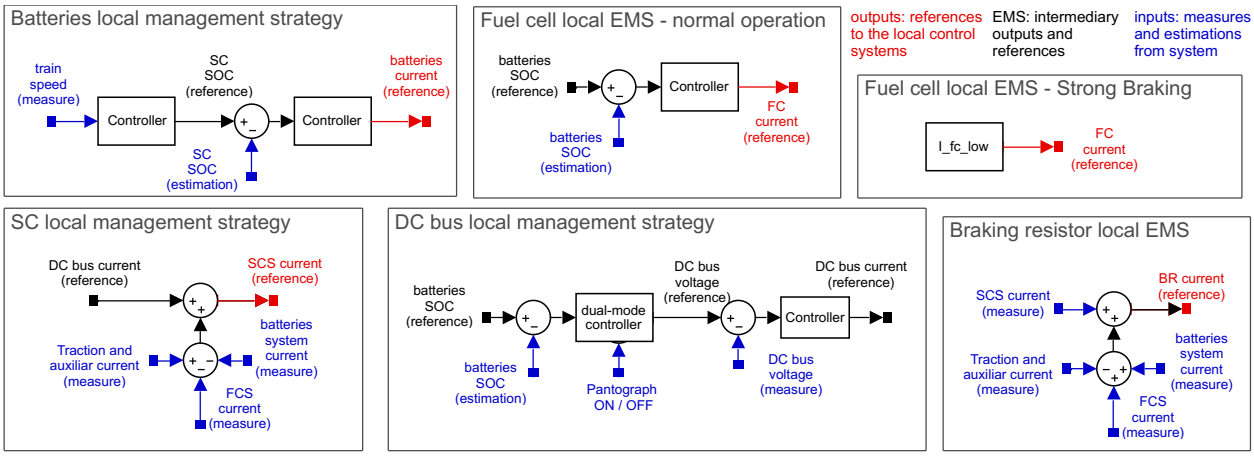

Figure 3. Ragone plot and energy flow between the locomotive's sources

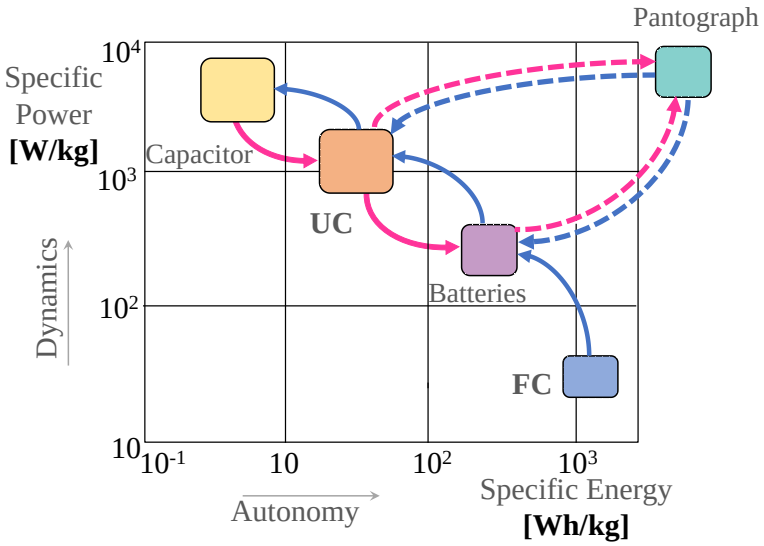

The guidelines listed below are proposed to define the EMS rules.

- The FC and the pantograph recharge the batteries.
- The batteries regulates the SC SOC.
- The SC regulates the DC bus voltage.

- The braking resistor use must be avoided.

Compared with the previous EMS presented in Mendoza et al. (2019), this one is oriented to reduce the energy consumed in the braking resistor. Two sets of rules are used to reach this objective. The first one rapidly decreases the output power of the fuel cell when braking is detected. The second set of rules allows using the DC bus capacitor to store part of the braking energy. The local energy management strategies allowing reaching the proposed objectives are presented in the next sections .

3.2. Fuel Cell local energy management strategy

The FC is the primary energy source embedded in the locomotive. As the FC has strong constraints to fast changes in the supplied current, its local EMS doesn't consider information about the current consumed by the loads or provided by the sources. The degradation is fast accelerated when turning the FC off and on again.

In normal operation, the FC only objective is to regulate the batteries SOC. The reference for its current $i_{fcS_{ref}}$ will increase with the reduction on the batteries measured state-of-charge SOC_b compared with an static reference $SOC_{b_{ref}}$. Here, this reference is constant and considered an optimization parameter. This SOC regulation is performed by a proportional controller, with K_{fc} gain.

The proportional controller is used to define the fuel cell current reference $i_{fc_{ref}}$ considering the error between the batteries state-of-charge SOC_b and its reference $SOC_{b_{ref}}$. Figure 4 illustrates $i_{fc_{ref}}$ for three different values for K_{fc}. Here, K_{fc_1} is the maximal and K_{fc_3} is the minimal feasible value for the controller gain.

A second operation mode is considered when the locomotive is braking fast. This is when a

Figure 4. Static reference for $i_{fc_{ref}}$

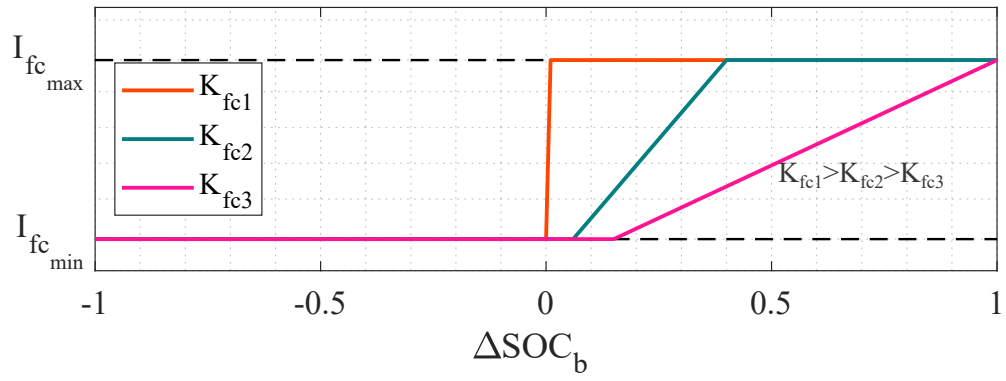

negative acceleration a_{loco} goes below a predetermined value a_{min}. In this operation mode, regenerative braking is activated, and the batteries and the SC are expected to operate at maximal recharge current. To avoid, or at least reduce, the dissipation of energy in the braking resistor, during strong braking detection (SBD), the fuel cell current reference is fast reduced to a low value $I_{fc_{low}}$. The Figure 5 presents the strategy behavior in the second operation mode, for a speed profile example. Additionally, due to the high degradation cost, the EMS must prevent the fuel cell to turns off as possible, and the current reference is then limited by a lower bound $I_{fc_{low}}$. Finally, the FC current must respect the static $I_{fc_{max}}$ and dynamic $dI_{fc_{max}}$ limits defined by the characteristics of the source. The fuel cell reference current is computed using Algorithm 1.

Figure 5. Second operation mode for $i_{fc_{ref}}$

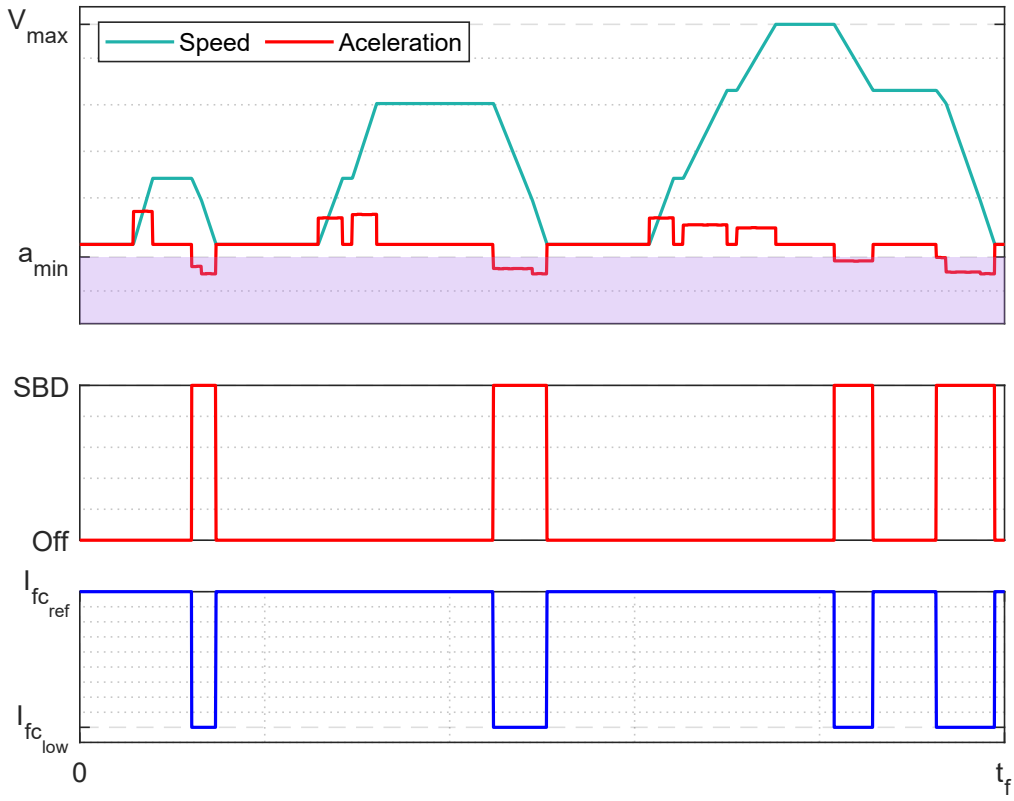

Algorithm 1: FC local EMS

Result: Define $i_{fcS_{ref}}$

read FC parameters: $I_{fc_{max}}$, $dI_{fc_{max}}$

read FC EMS parameters: K_{fc}, $SoC_{b_{ref}}$, $I_{fc_{low}}$, a_{min}

read measures: SOC_b, i_{fc}, a_{loco}

if $a_{loco} \leq a_{min}$ **then**
  $i_{fc_{ref}}* = I_{fc_{low}}$
else
  $i_{fc_{ref}}** = K_{fc}(SOC_{b_{ref}} - SOC_b)$
  $i_{fc_{ref}}* = max(I_{fc_{low}}, min(I_{fc_{max}}, i_{fc_{ref}}**))$
end

if $i_{fc_{ref}}* \geq i_{fc} + dI_{fc_{max}}$ **then**
  $i_{fc_{ref}} = i_{fc} + dI_{fc_{max}}$
else
  $i_{fc_{ref}} = i_{fc_{ref}}*$
end
if $i_{fc_{ref}}* \leq i_{fc} - dI_{fc_{max}}$ **then**
  $i_{fc_{ref}} = i_{fc} - dI_{fc_{max}}$
else
  $i_{fc_{ref}} = i_{fcS_{ref}}*$
end

3.3. Batteries local energy management strategy

The batteries transfer energy from the fuel cell to the supercapacitors. This condition is mandatory to ensure the SC system can operate as the main power transitory source. The batteries don't have the same dynamic limitations as the FC and can be used as a power source and in less degree for regenerative braking. The reference for its current $i_{b_{ref}}$ increases if the SC state-of-charge SOC_{sc} decreases compared with a dynamic reference $SOC_{sc_{ref}}$. This control is performed using a proportional controller with K_b gain and is shown in Figure 6. Here, K_{b_1} is the maximal and K_{b_3} is the minimal feasible value for the controller gain.

Several researches suggest to define a dynamic reference for the supercapacitor state-of-charge considering the speed and kinetic energy of the vehicle Solano et al. (2011); Ciccarelli et al. (2012); Iannuzzi and Tricoli (2012); Allègre et al. (2010). The reference for the SC state of charge ($SOC_{sc_{ref}}$) depends on the train speed: at maximal speed Vel_{max} the SC are discharged to a minimal state of charge ($SOC_{sc_{Velmax}}$): this enables enough place to store the energy recovered by the regenerative braking hence minimizing the risk of using the braking resistor. When the locomotive is stopped, the UC are recharged until a maximal state of charge ($SOC_{sc_{Vel0}}$), and this enables enough energy in the SC to support accelerating the train.

A proportional controller is used to define $SOC_{sc_{ref}}$: a decreasing function of the train speed, which is directly related to the kinetic energy of the train. This controller is illustrated in Figure 7. The batteries local EMS does not consider the power consumed by the load or provided by the other sources.

The batteries reference current is computed using Algorithm 2.

Figure 6. Reference for $i_{b_{ref}}(t)$

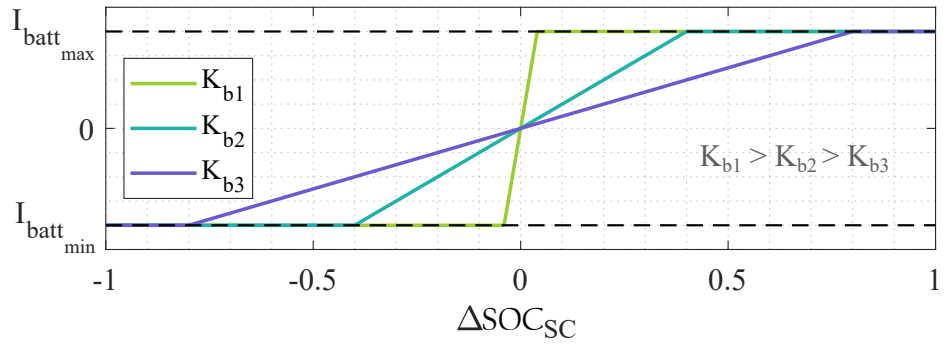

Figure 7. Reference for $SOC_{sc_{ref}}$

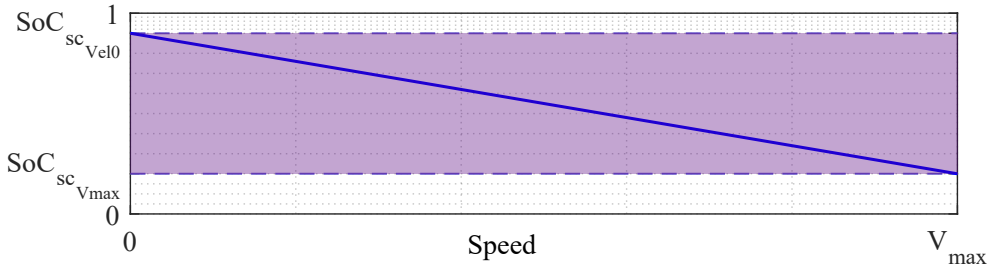

Algorithm 2: Batteries Local EMS

Result: Define $i_{bS_{ref}}$

read batteries parameters: $I_{batt_{max}}$, $I_{batt_{min}}$

read EMS parameters: $SOC_{sc_{Vel0}}$, $SoC_{sc_{Vel_{max}}}$, Vel_{max}

read measures: SOC_{sc}, Vel_{loco}

$SoC_{sc_{ref}} = SOC_{sc_{Vel0}} - \frac{Vel_{loco}}{Vel_{max}}(SOC_{sc_{Vel0}} - SOC_{sc_{Vel_{max}}})$

$i_{bS_{ref}}* = K_b(SOC_{sc_{ref}} - SOC_{sc})$

$i_{bS_{ref}} = max(I_{batt_{min}}, min(I_{batt_{max}}, i_{bS_{ref}}*))$

3.4. Supercapacitors local EMS

The SC system balances the currents consumed by the locomotive and provided by the FC system and batteries system. Additionally, the SC system regulates the DC bus voltage level, supplying a regulation current i_{bus}. The algorithm to define this current is presented in the next subsection.

As the SCS balance the currents supplied and consumed by the loads, the SC EMS only uses currents as inputs. Additionally, and compared with the FC and batteries, the UC system reference current $i_{scS_{ref}}$ is the only reference directly computed at the DC bus level side. The UC system reference current is computed using Algorithm 3.

Algorithm 3: Supercapacitors Local EMS

Result: Define $i_{sc_{ref}}$

read SC parameters:$I_{scs_{max}}$, $I_{scs_{min}}$

read control references: $I_{bus_{ref}}$

read measures: i_{tr}, i_{aux}, i_{fcS}, i_{bS}

$i^*_{scS_{ref}} = i_{bus_{ref}} + i_{tr} + i_{aux} - i_{fcS} - i_{bS}$

$i_{scS_{ref}} = max(I_{scs_{min}}, min(I_{scs_{max}}, i^*_{scS_{ref}}))$

3.5. Braking resistor local energy management strategy

A braking resistor is implemented in the locomotive. It is modeled as a perfectly controllable current source Lhomme et al. (2018a). The braking resistor use must be minimized. However, during braking, the excess of power that cannot be stored in the SC and batteries should be sent to the braking resistor to avoid overvoltages in the DC bus. This local EMS has no parameters. The braking resistor reference current $i_{br_{ref}}$ is computed using Algorithm 4.

Algorithm 4: Braking resistor Local EMS

Result: Define $i_{br_{ref}}$

read measures: i_{tr}, i_{aux}, i_{fcS}, i_{bS}, i_{scS}

$i^*_{br_{ref}} = i_{tr} + i_{aux} - i_{fcS} - i_{bS} - i_{scS}$

$i_{br_{ref}} = max(0, i^*_{br_{ref}}))$

3.6. DC Bus energy management strategy

The DC bus voltage local energy management strategy depends on the presence or not of the pantograph. The main difference between the two operations modes is the reference for the DC bus operation voltage. The DC bus voltage level depends on the energy supplied to/from the DC bus capacitor. A regulation current $i_{bus}(t)$ can be supplied to/from the capacitor to control the DC bus voltage. As the capacitor current depends on the balance showed in Equation 1, and the DC bus capacitor has not a power converter, this current has to be indirectly controlled. To keep the DC bus voltage constant, $i_{bus}(t)$ in Equation 1 is set to zero. Then the UCS balance the current supplied by the sources and consumed by the loads. To increase/decrease the DC bus voltage, the UCS provides more/less current than required in this balance. This excess of current $i_{bus}(t)$ is supplied by the DC bus capacitor and increases/decreases the DC bus voltage. A proportional controller is used to determine the reference value for $i_{bus}(t)$. The input of this controller is the difference between the DC bus voltage reference $v_{bus_{ref}}$ and measure $v_{bus}(t)$. With or without pantograph, only one proportional controller with K_{bus} gain is implemented. This controller is illustrated in Figure 9

Figure 8. Reference for $i_{bus_{ref}}$

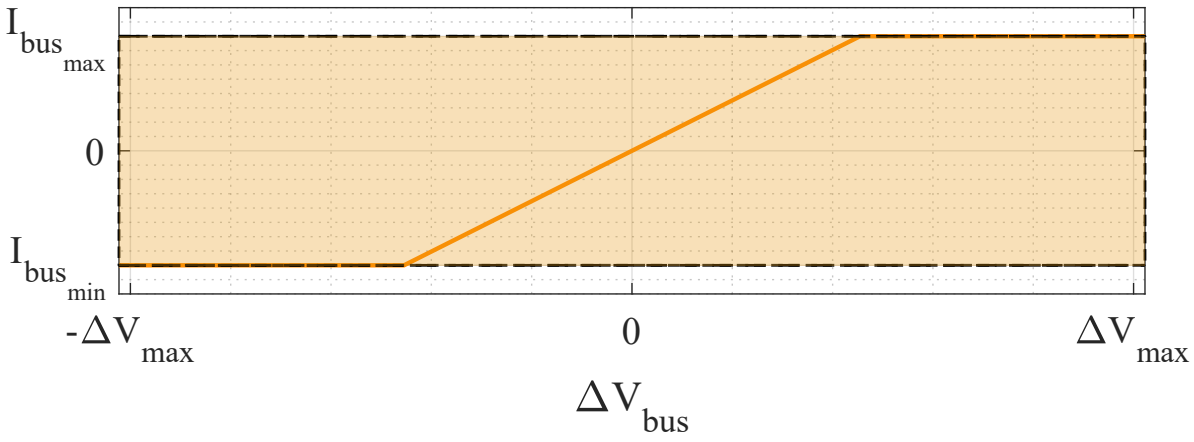

Figure 9. Reference for $i_{bus_{ref}}$

3.6.1. Mode Pantograph ON

The pantograph is a secondary source that can be eventually used to supply power to recharge the batteries. The energy from the pantograph cannot be directly controlled. This is indirectly done by controlling the DC bus voltage, as explained before. If the DC bus voltage is lower than the pantograph voltage, the power flows from the network to the locomotive. If the DC bus voltage has the same magnitude of the pantograph, the flow of power will be zero.

If the batteries are charged, the DC bus voltage reference $v_{bus_{ref}}$ is set to the same value of the pantograph voltage V_{line}. When the batteries are discharged, and its SOC goes beyond a low boundary $SOC_{b_{low}}$, the DC bus voltage reference $v_{bus_{ref}}$ is set to a lower value, to consume power from the pantograph. In this research work, the pantograph supplies a constant current I_{rech}.

3.6.2. Mode Pantograph OFF

The DC bus capacitor can store a limited amount of energy during strong braking. When the train is in normal operation $v_{bus_{ref}}$ is set to a low value V_{low}. This voltage should respect the restrictions of the DC bus.

When strong braking is detected, $v_{bus_{ref}}$ is set to a high value V_{high}. This condition allows storing some of the braking energy in the capacitor. The DC bus voltage regulation current reference is computed using Algorithm 5.

Algorithm 5: Local DC Bus Capacitor EMS

Result: Define $i_{bus_{ref}}$

read DC bus/pantograph parameters: $R_{panto}, V_{line}, I_{bus_{low}}, I_{bus_{high}}$

read EMS parameters: $SOC_{b_{low}}, I_{rech}, V_{high}, V_{low}, a_{min}$

read measures: SOC_b, V_{bus}, $a_{loco}, Pantograph_{ON}$

if *pantograph ON* **then**

  if $SOC_b > SOC_{b_{low}}$ **then**

    $v_{bus_{ref}}(t) = V_{line}$

  else

    $v_{bus_{ref}}(t) = V_{line} - R_{panto} I_{rech}$

  end

else

  if $a_{loco} \leq a_{min}$ **then**

    $v_{bus_{ref}}(t) = V_{high}$

  else

    $v_{bus_{ref}}(t) = V_{low}$

  end

end

$I_{bus_{ref}}* = K_{bus}(V_{bus_{ref}} - V_{bus})$ $I_{bus_{ref}} = max(I_{bus_{low}}, min(I_{bus_{max}}, I_{bus_{ref}}*))$

3.7. Dual-mode EMS and parameters

Figure 2 illustrates the global EMS for the dual-mode locomotive. This strategy requires defining two sets of parameters. The first subset of parameters is related to the sources characteristics and constraints *e.g.* the maximal current. The second set of parameters is related to the local EMS for each source *e.g.* the proportional controllers gains.

The first subset has 9 parameters: the maximal FC current $I_{fc_{max}}$, the maximal change of the FC current in a computing period $dI_{fc_{max}}$, the maximal batteries current $I_{batt_{max}}$, the minimal batteries current $I_{batt_{min}}$, the maximal SC current, the minimal SC current, the maximal locomotive speed Vel_{max}, the pantograph resistance R_{panto} and the network voltage V_{line}.

The subset related to the local EMS has 14 parameters: 3 for the local FC EMS, 7 for the local DC bus EMS, 3 for the local batteries EMS and the acceleration to identify Strong braking a_{min}.

The local FC EMS requires the proportional gain K_{fc}, the minimal FC current $I_{fc_{low}}$, and the batteries SOC reference $SOC_{bat_{ref}}$. The local batteries EMS requires: the SC SOC reference at maximal locomotive speed $SOC_{sc_{Velmax}}$, the SC SOC reference when locomotive stopped $SOC_{sc_{Vel0}}$ and the proportional gain K_b.

The local DC bus EMS requires the maximal $I_{bus_{high}}$ and minimal $I_{bus_{low}}$ bus current, the constant pantograph current I_{rech}, the proportional gain K_{bus}, the batteries SOC reference for start pantograph recharge $SOC_{b_{low}}$ and the voltage references for normal operation V_{low} and strong braking

without pantograph V_{high}.

4. EMS parameters Selection

For any load profile, an optimal set of EMS parameters should minimize the cost function presented in Section 2.2 and respect the constraints defined in Section 2.1. With all the EMS parameters listed, the next challenge is to identify their optimal values. Some authors use heuristic or analytical optimization techniques to determine sets of optimal EMS parameters. These sets can be optimal for a determined profile but not optimal for every possible profile. This tuning process strongly depends on the problem specifications. However, optimizing any EMS for these evaluation profiles doesn't guarantee optimally for an unknown scoring profile.

4.1. EMS parameters tuning

In this research work a simple methodology to determine the EMS parameters. This methodology is inspired by the experimental method Friedman et al. (1994); Wagner et al. (2014), and the Taguchi approach Taguchi and Phadke (1989). It is a systematic approach to understand how EMS parameters affect the system dynamics and cost functions. The proposed method consists of evaluating in a feasible space of solutions several sets of parameters.

The main set of parameters W_{EMS} is composed of subsets of feasible solutions for each parameter

$$W_{EMS} = \{w_1, w_2, w_3, \ldots, w_m\}$$

Each parameter subset w_i is composed of x_i levels (feasible solutions). These subsets are defined using the following methodology:

First, boundaries for each of the EMS parameters are defined. It is necessary to carefully select lower and higher limits ($w_{i_{low}}$ and $w_{i_{high}}$) to generate a feasible search space.

Then the x_i levels for each parameter are determined. This number could be different for each parameter. The subsets with feasible values are generated as illustrated below:

$$w_i \rightarrow \underbrace{\{w_{i_1}, w_{i_2}, w_{i_3}, \ldots w_{i_n}\}}_{\text{feasible solutions range}}$$

with $w_{i_1} = w_{i_{low}}$ and $w_{i_n} = w_{i_{high}}$

Finally, a full factorial experiment is performed. It is an exhaustive research of all the feasible combinations of levels for each parameter (solutions). This experiment requires S_N simulations given by

$$S_N = \prod_{i=1}^{m} x_i \tag{17}$$

where m is the total number of parameters.

The figure 10 presents the case when the parameters set to optimize is

$$W_{EMS} = \{A, B, C, D\}$$

Then the high and low limits are defined in a feasible space for each parameter

$$A \rightarrow A_{\text{low}} = A_1, \quad A_{\text{high}} = A_2$$

$$B \rightarrow B_{\text{low}} = B_1, \quad B_{\text{high}} = B_3$$

$$C \rightarrow C_{\text{low}} = C_1, \quad C_{\text{high}} = C_3$$

$$D \rightarrow D_{\text{low}} = D_1, \quad D_{\text{high}} = D_3$$

Considering the limits *low* and *high*, the number of levels for each parameter is chosen. It means the values between the limits for testing. For the A parameter case, there are selected two levels. For the cases of B, C, D, three levels are chosen. The parameters sets generated, taking into account the search space, are presented in Figure 10. The parameters set that corresponds to the Simulation 1 is given by $\{A_1, B_1, C_1, D_1\}$.

For example, in the case of Simulation 43, the parameters set organized to do the simulation is $\{A_2, B_2, C_3, D_1\}$. The simulations number for this feasible search space is given by the equation (17), and this is

$$S_N = x_A \cdot x_B \cdot x_C \cdot x_D$$

$$S_N = 2 \cdot 3 \cdot 3 \cdot 3 = 54$$

In the dual-mode locomotive EMS parameters search, a full fractional experiment is performed for each consumption profile provided for IEEE VTS Motor Vehicles Challenge 2019 organizers.

Then in each experiment, for each simulation, a Total Cost value is obtained. For Figure 10, 54 different Total Cost values and 54 different Energy Wasted in the Braking Resistor values are obtained. The next step consists of selecting the parameters set that provide the less Total Cost and the less Energy Wasted in the Braking Resistor.

Notably, as a full fractional experiment is done for each consume profile, a single set of parameters must be selected under the less Total Cost and the Energy Wasted in the Braking Resistor conditions. The results obtained for each speed profile are presented in the Appendix 1. This is done to guarantee the versatile of the strategy for any power consumption profile, and especially for unknown power profiles used to evaluate the EMS.

The computational cost of this method could be prohibitive when the number of solutions increases. Simultaneous optimization of all the parameters will exponentially increase the number of solutions. An alternative iterative algorithm is used to reduce the computational cost. The optimizable parameters are divided into two groups. In a first step, the FC local EMS and batteries local EMS are simultaneously optimized with the other parameters constant. After this, in a second step, the DC bus local EMS parameters are optimized, keeping the other parameters constant. This process is repeated until the best solution between successive iterations has not a significant improvement. The output of this methodology can be considered as a set of near-optimal parameters

for the proposed EMS.

5. Validation results

The proposed EMS is evaluated by simulations using the dual-mode locomotive model, and speed and bus power profiles provided by the IEEE VTS motor vehicles challenge 2019 organizers Lhomme et al. (2018a).

Following the rules and the IEEE VTS Motor Vehicles Challenge's philosophy, the three profiles presented in Lhomme et al. (2018a) are used to tune the EMS. This tuning is performed following the methodology presented in Section 2.10. A fourth power profile, provided by the organizers of the IEEE VTS Motor Vehicles Challenge 2020, is used to evaluate the EMS. This profile was unknown to the challenge participants and is not used to tune the EMS. The scoring profiles are illustrated in Figure 11. All the solutions must respect the constraints in Table 1. Two study cases are presented, the two cases use the same sources model and power profiles, but they consider two different hydrogen consumption models illustrated in Figure 14.

Each one of the considered study cases has a specific purpose: the first evaluation aims to highlight the principal contributions of the EMS, compared with the EMS proposed in Mendoza et al. (2019). The second evaluation main objective is to demonstrate that the proposed strategy can almost eliminate the necessity to use the braking resistor and then maximize the energy recovered using regenerative braking.

Table 1
Constraints

Parameter (constraints)	**Value**
FC maximal current	1400[A]
FC maximal current rate change	50[A/s]
FCS maximal power	500[kW]
Batteries maximal SOC	1
Batteries minimal SOC	0.2
Batteries maximal current (discharge)	3200 [A]
Batteries minimal current (charge)	800 [A]
Batteries maximal power	2[MW]
SC maximal SOC	1
SC minimal SOC	0.35
SC maximal current (charge & discharge)	1900 [A]
SC maximal power	2[MW]

Figure 10. Full Fractional Experiment Performance

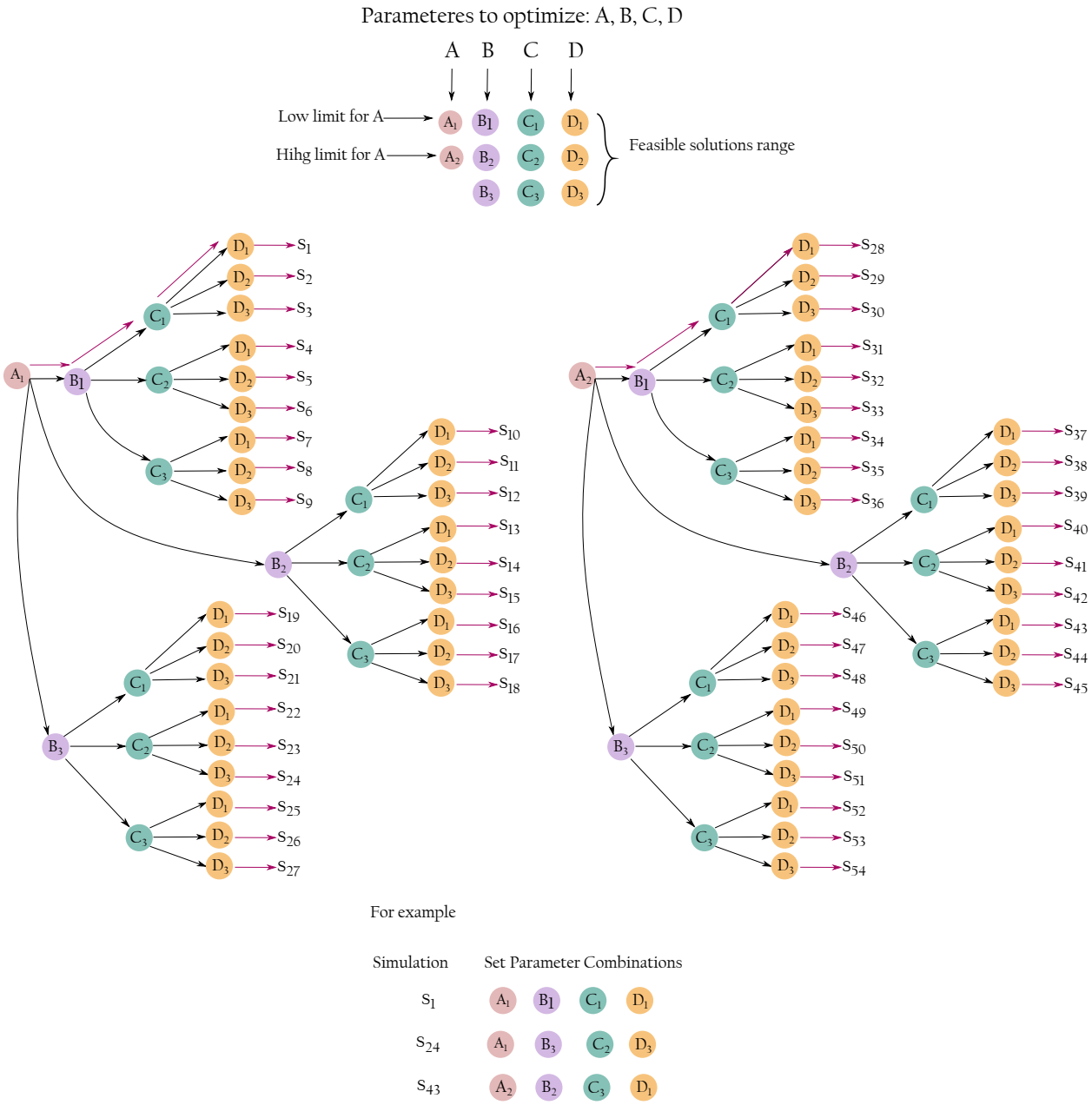

Figure 11. Traction + auxiliaries power and Speed profile

5.1. First H_2 consumption model

For the first validation scenario, the cost function defined in Lhomme et al. (2018a). The simulation results are compared with the proposed by Mendoza et al. (2019). These results are not optimal, but they were the best solution submitted to the IEEE VTS motor vehicles challenge 2019.

The methodology in Section 4.1 is used to find a set of parameters of the EMS. Figures 12 presents the best results submitted to the IEEE VTS Motors Vehicles Challenge 2019. Figures 13, illustrates the results obtained with the new EMS. The total cost is 6.03€ for the original EMS and 1.21€ for the new EMS. The original EMS has a braking resistor energy consumption of 3.03 kWh. The improved strategy has a braking resistor energy consumption of 2.85 kWh.

In both EMS, the FC starts operating in a high power zone to recharge the batteries until the desired state-of-charge. After this, the fuel cell operates in a high-efficiency zone, keeping the batteries charged. In the new EMS, when strong braking is detected, the fuel cell power decreases its output power, at the maximal rate, to reduce the necessity to use the braking resistor. Eliminating this waste of energy is, however, only possible when the fuel cell operates in a high-efficiency zone. In this specific study case, after the first hour needed to recharge the batteries. The high difference observed in the total cost obtained with the two EMS is mainly due to the sustainability cost, because the energy stored in the batteries at the end of the mission is much higher in the new strategy.

It has been demonstrated with this first study case that a considerable reduction in the total cost of the mission can be obtained using the new EMS. The work presented in Jia et al. (2019) proposes a rule-based EMS where the FC operates supplying high power all the time. This power is used to recharge the SC and batteries to their maximal SOC. In this strategy, the total cost is even negative -4.69€.

In the scoring cycle, the locomotive is driven for 70.86 km during more than two hours. The locomotive and its ancillaries consume around 260 kWh. Using the model provided by Lhomme et al. (2018a), the hydrogen consumption is 88 grams with the proposed EMS, and 90 and 178 for the EMS in Mendoza et al. (2019) and Jia et al. (2019) respectively. These results are not realistic: one gram of hydrogen stores about 0.04 kWh. A FC with 50 % (high) average efficiency consumes around 50g H_2 to produce one electrical kWh. Around 13kg of H_2 are needed to supply the energy consumed by the locomotive. Additional H_2 is required to provide the system energy losses and to recharge the SC and batteries. As the H_2 consumption is underestimated, the equivalent cost of energy produced by the fuel cell is very low compared with the expected in a realistic fuel cell. With this consumption model, it is better to use the fuel cell to produce energy to recharge the batteries and SC. For this reason, the solutions presented by Jia et al. (2019) or Mendoza et al. (2019) operate the FC close to the maximal power and were the best solutions to the IEEE VTS motor vehicles challenge 2019.

Figure 12. IEEE VTS Motors Vehicles Challenge 2019 best solution

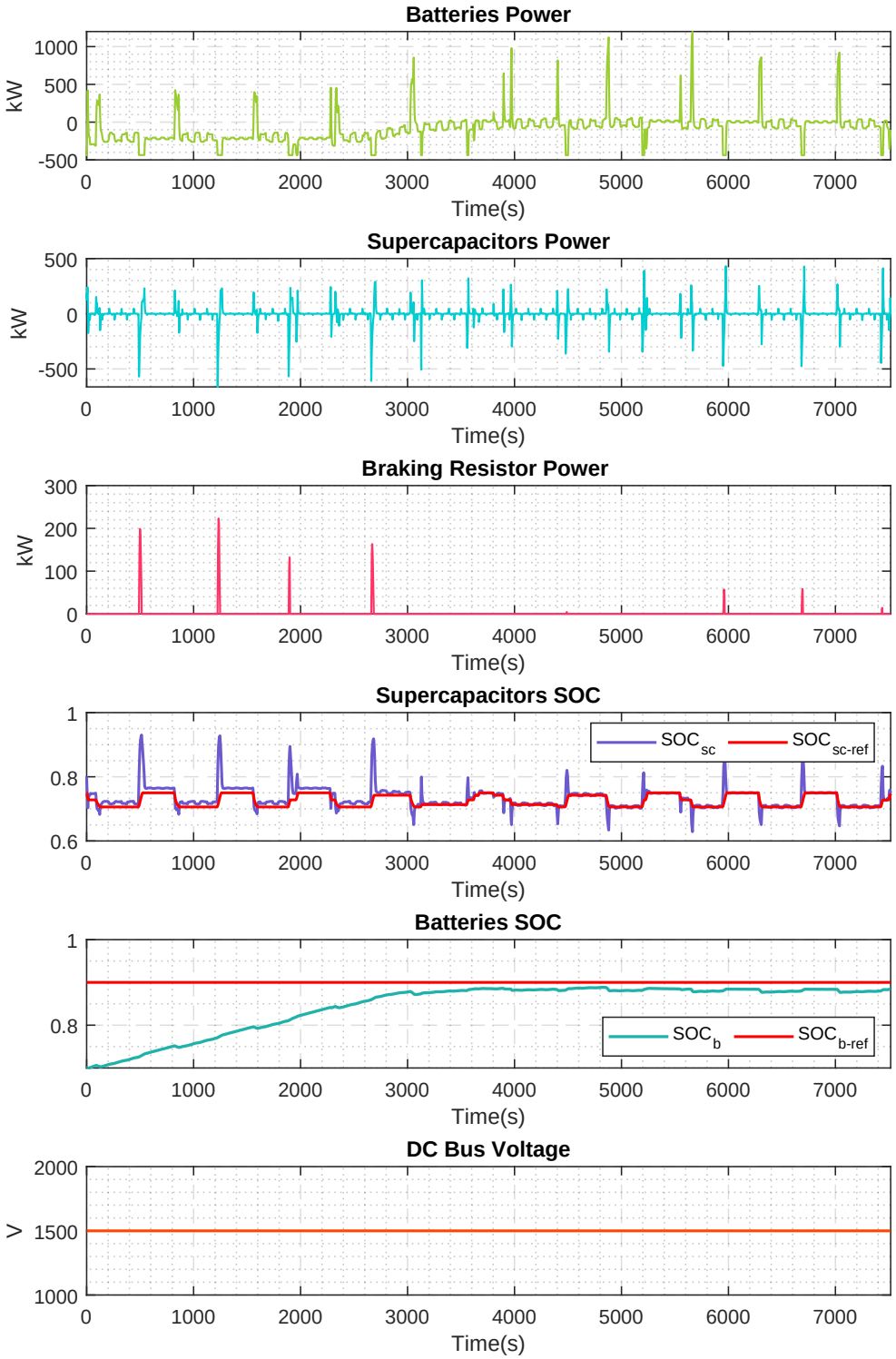

Figure 13. IEEE VTS Motors Vehicles Challenge 2019 - new EMS

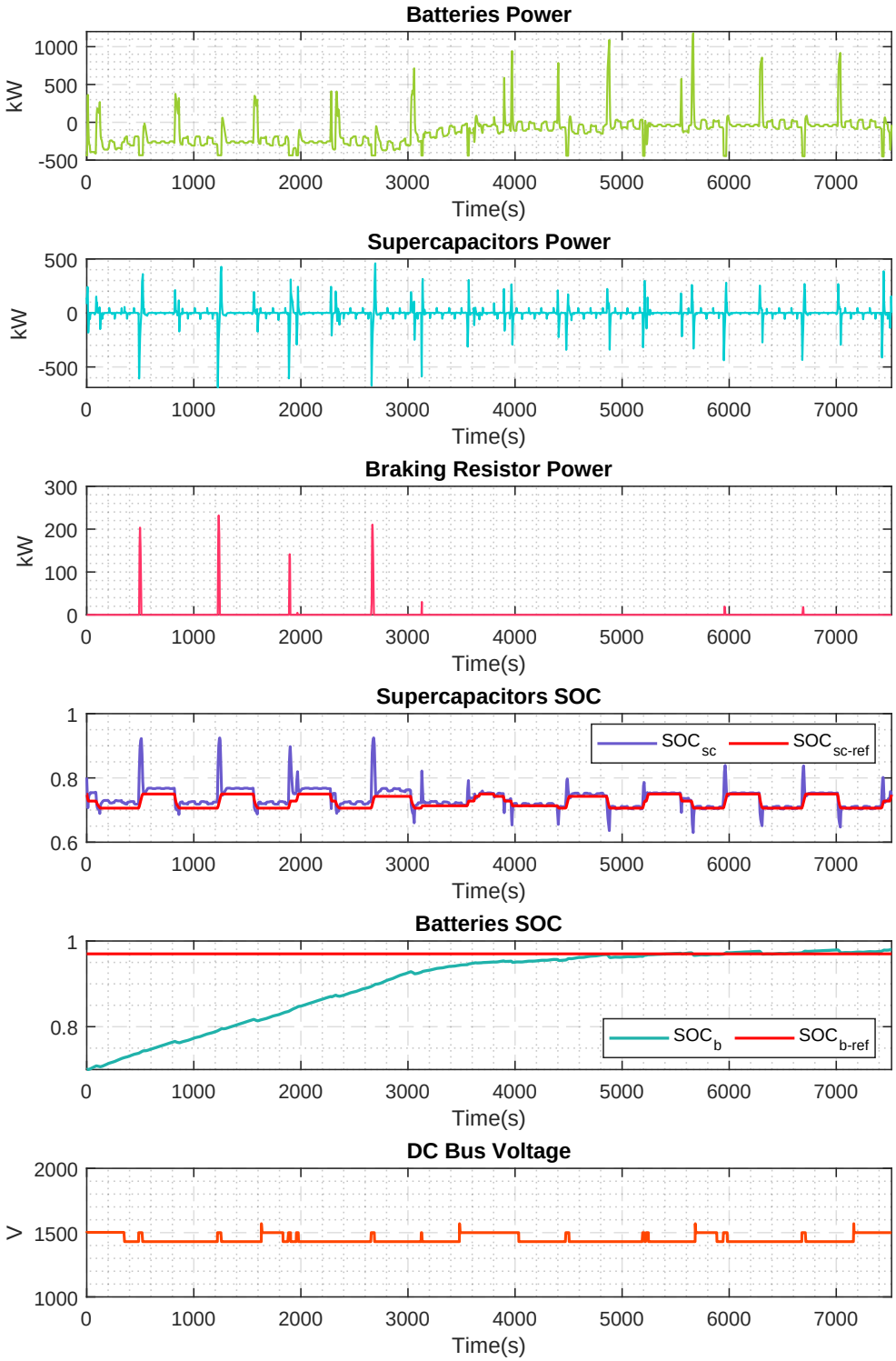

5.2. Second H_2 consumption model

A second evaluation of the EMS is performed using the same speed and bus power profile but a different H_2 consumption model, the Figure 14 compares the two different hydrogen comsumption models . The new model is inspired by the proposed in IEEE VTS Motors Vehicles Challenge 2017. The model for calculating the cost of recharging at the end of the cycle was changed. The equation (16) was replaced by the equation (18).

$$\varepsilon_{sust2} = \frac{\mathrm{N_{cost}}}{10^3} \left(\Delta \mathrm{SOC_b E_{b}}_{rate} + \Delta \mathrm{SOC_{sc} E}_{sc_{rate}}\right) \tag{18}$$

where,

$$\Delta \mathrm{SOC_b} = \mathrm{SOC_{b_{init}}} - \mathrm{SOC_{b_{meas}}}$$

$$\Delta \mathrm{SOC_{sc}} = \mathrm{SOC_{sc_{init}}} - \mathrm{SOC_{sc_{meas}}}$$

Figure 14. H_2 flow models

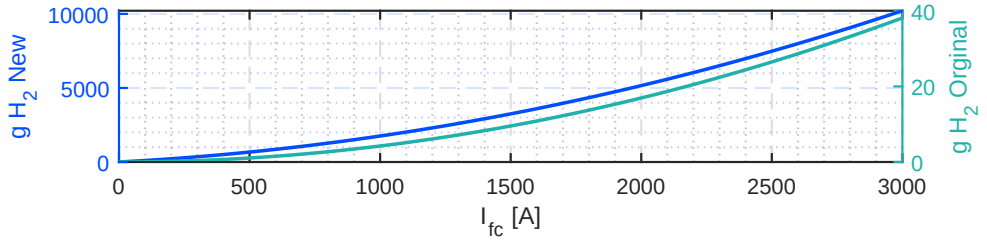

The methodology proposed in Section 4.1 is used to find a set of parameters of the proposed EMS. Figure 15 illustrates the results obtained with the new H_2 consumption model. The new

total cost is 57.56€ and 14 kg of H_2. In this case, the fuel cell operates in a high power zone to recharge the batteries until the desired state-of-charge. However, the desired SOC with this strategy is much lower than with the previous EMS, and the fuel cell will work in this operation mode only for a few minutes compared with one hour in the previous study case. When strong braking is detected, the FC power decreases at its minimal power at the maximal rate, to reduce the necessity to use the braking resistor. As the fuel cell does not operate a long time in high power mode, the energy dissipated in the braking resistor is almost eliminated. The proposed DC bus voltage regulation strategy allows recovering part of the braking energy. The energy consumed in the braking resistor is 0.064 kWh, around 50 times less than the energy dissipated with the previous EMS. This reduction is illustrated in Figure 16. Table 2 summarizes the results obtained with the new strategy and compare it with the results obtained with the old strategy, in terms of recovery of braking energy. It is demonstrated here that using this EMS, the energy recovered in braking can be improved. Considering the efficiency of the FC, and the energy consumed by the load, the optimal consumption should be around 13kg of H_2. These results confirm that using the proposed EMS, and the results are close to the expected optimal values.

Table 2
Results

Variables	**Original EMS**	**New EMS**
Recovered braking energy [%]	91.5	99.8
Energy consumption reduction[%]	11.7	12.8

Figure 15. New H_2 consumption model - New EMS

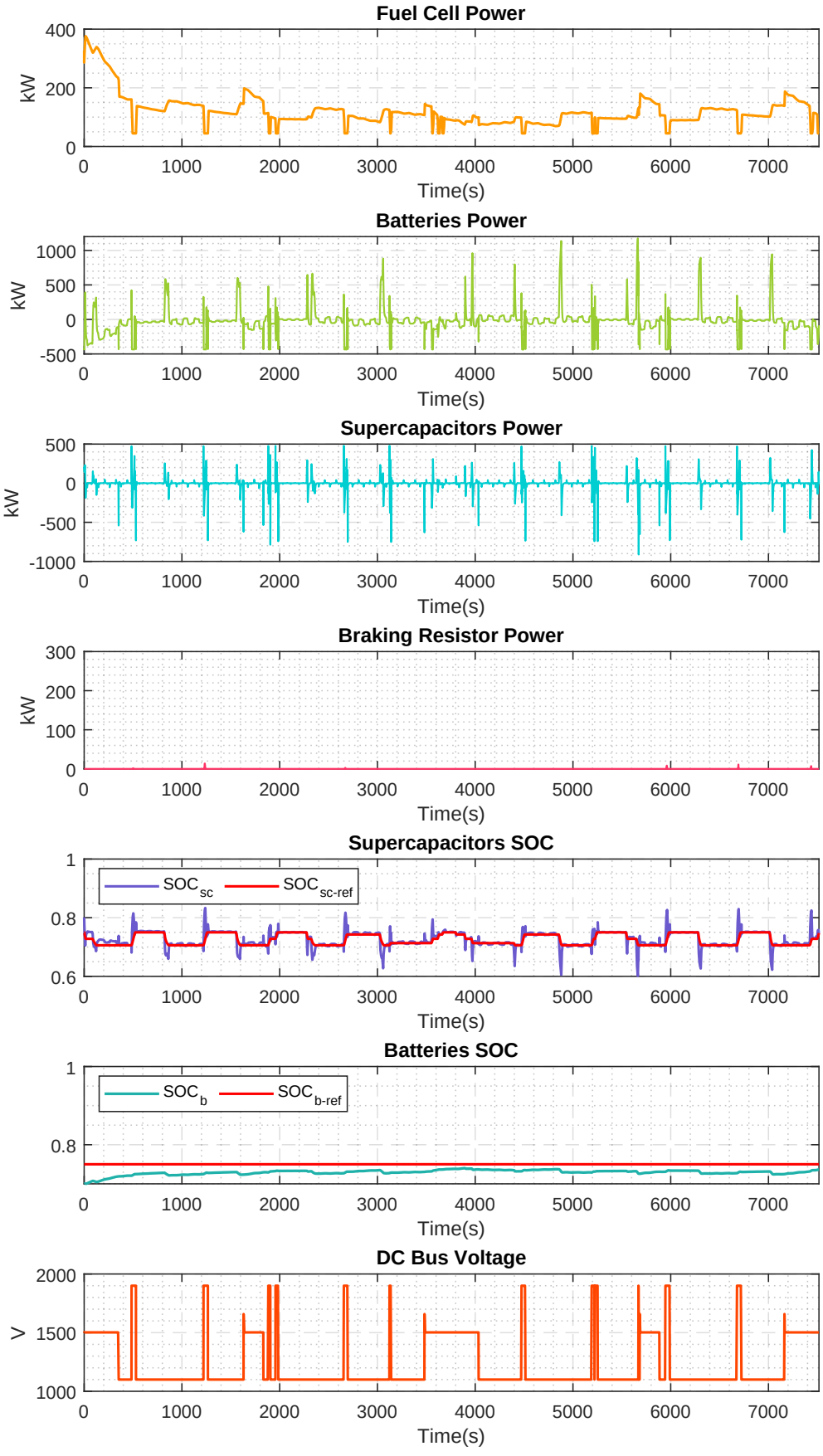

Figure 16. Braking resistor power

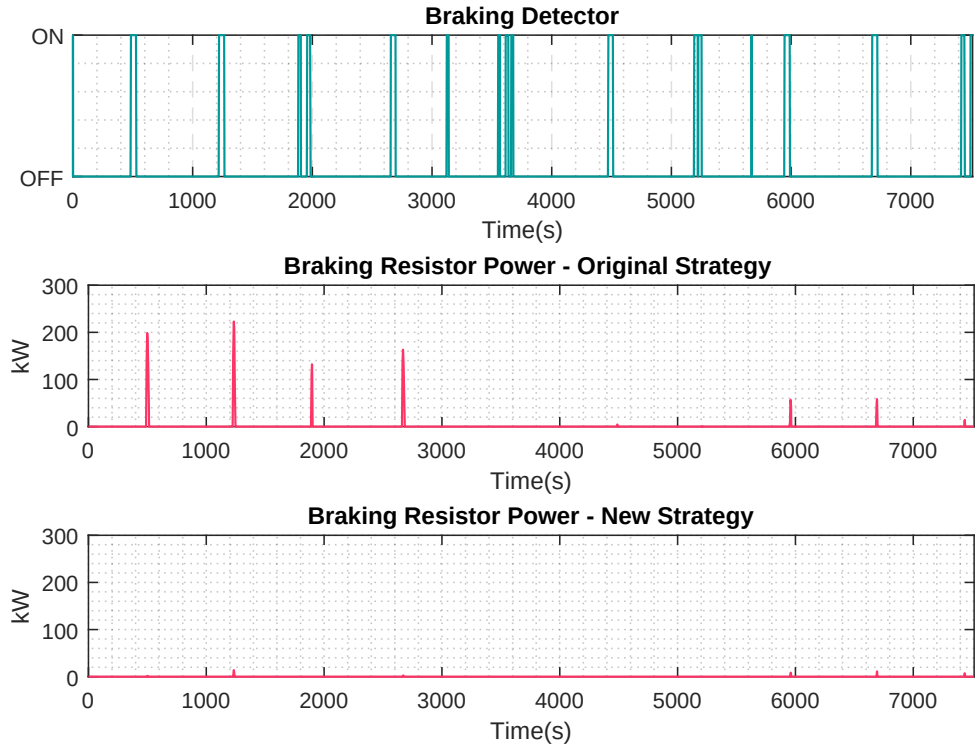

5.3. Conclusion

This master thesis proposed an EMS to define power distribution references in a dual-mode locomotive equipped with a FC system, a SC system, batteries, a braking resistor and intermittent access to a DC electrified overhead line. The solution proposed is a rule-based approach inspired on the Ragone plot. The proposed EMS is relatively simple and conceived to be intuitive and easy to implement. The master thesis also introduces a simple methodology to tune the EMS parameters. As illustrated with the two study cases, the parameters of the EMS strongly depends on the problem characteristics, such as the price of the electricity from the network or the hydrogen.

As the EMS has a low number of parameters, future research can scope on improving the

tuning procedure, using optimization techniques such as genetic algorithms. New research should also focus on including GPS information in the EMS: anticipating potential energy gains at negative slope profiles, the SC and batteries SOC references can be modified to enable recovering this energy. Even if the results are not optimal, this strategy is straightforward to implement and could be easily adapted to be used in other FC-UC-Batt hybrid sources.

In the study case, up to 99.8 % of the braking energy in a freight train can be recovered. This saving represents a 8.3 % increase of the energy recovered and 1.1 % of the total energy consumption, compared with the work presented in Mendoza et al. (2019). The global energy consumption reduction in these trains is estimated by 12.8 % using UC. These results suggest that in applications with a higher frequency of start/stops like metro trains or tramways, this reduction could be even more than 30 %. This demonstrates, that using a well designed EMS, the energy recovered during braking in embedded energy sources can be highly increased and almost eliminate the necessity to dissipate energy in braking resistors.

Acknowledgement

This research was partially funded by the Emerging Leaders in the Americas Program (ELAP) from the Government of Canada and for the Electrical, Electronic and Telecommunications school from Universidad Industrial de Santander.

References

Albrecht, A., Howlett, P., Pudney, P., Vu, X., and Zhou, P. (2016). The key principles of optimal train controlPart 1: Formulation of the model, strategies of optimal type, evolutionary lines, location of optimal switching points. *Transportation Research Part B: Methodological*, 94:482–508.

Allègre, A. L., Bouscayrol, A., Delarue, P., Barrade, P., Chattot, E., and El-Fassi, S. (2010). Energy storage system with supercapacitor for an innovative subway. *IEEE Transactions on Industrial Electronics*, 57(12):4001–4012.

Babazadeh, H., Asghari, B., and Sharma, R. (2014). A new control scheme in a multi-battery management system for expanding microgrids. In *ISGT 2014*, pages 1–5. IEEE.

Baert, J., Jemei, S., Chamagne, D., Hissel, D., Hibon, S., and Hegy, D. (2013). Energetic macroscopic representation of a hybrid electric locomotive and experimental characterization of nickel-cadmium battery cells. In *15th European Conference on Power Electronics and Applications (EPE)*, pages 1–10. IEEE.

Barrero, R., Van Mierlo, J., and Tackoen, X. (2008). Energy savings in public transport. *IEEE vehicular technology magazine*, 3(3):26–36.

Bocharnikov, Y., Tobias, A., Roberts, C., Hillmansen, S., and Goodman, C. (2007). Optimal driving

strategy for traction energy saving on dc suburban railways. *IET Electric Power Applications*, 1(5):675–682.

Chen, H., Pei, P., and Song, M. (2015). Lifetime prediction and the economic lifetime of Proton Exchange Membrane fuel cells. *Applied Energy*, 142:154–163.

Chymera, M., Renfrew, A., and Barnes, M. (2008). Analyzing the potential of energy storage on electrified transit systems. In *Proceedings of the 8th world congress of railway research*, pages 1–10.

Ciccarelli, F., Iannuzzi, D., and Tricoli, P. (2012). Control of metro-trains equipped with onboard supercapacitors for energy saving and reduction of power peak demand. *Transportation Research Part C: Emerging Technologies*, 24:36–49.

Cucala, A. P., Fernández, A., Sicre, C., and Domínguez, M. (2012). Fuzzy optimal schedule of high speed train operation to minimize energy consumption with uncertain delays and drivers behavioral response. *Engineering Applications of Artificial Intelligence*, 25(8):1548–1557.

Destraz, B., Barrade, P., Rufer, A., and Klohr, M. (2007). Study and simulation of the energy balance of an urban transportation network. In *2007 European conference on power electronics and applications*, pages 1–10. IEEE.

Din, T. and Hillmansen, S. (2018). Energy consumption and carbon dioxide emissions analysis for a concept design of a hydrogen hybrid railway vehicle. *IET Electrical Systems in Transportation*, 8(2):112–121.

Domínguez, M., Cucala, A., Fernández, A., Pecharromán, R., and Blanquer, J. (2011). Energy efficiency on train control: design of metro ato driving and impact of energy accumulation devices. In *9th World Congress of Railway Research*, pages 22–26.

Franke, R., Terwiesch, P., and Meyer, M. (2000). An algorithm for the optimal control of the driving of trains. *Proceedings of the IEEE Conference on Decision and Control*, 3:2123–2128.

Friedman, S., Friedman, D., and Sunder, S. (1994). *Experimental methods: A primer for economists*. Cambridge University Press.

González-Gil, A., Palacin, R., and Batty, P. (2013). Sustainable urban rail systems: Strategies and technologies for optimal management of regenerative braking energy. *Energy Conversion and Management*, 75:374–388.

González-Gil, A., Palacin, R., Batty, P., and Powell, J. P. (2014). A systems approach to reduce urban rail energy consumption. *Energy Conversion and Management*, 80:509–524.

Gordon, S. P. and Lehrer, D. G. (1998). Coordinated train control and energy management control strategies. *Proceedings of the IEEE/ASME Joint Railroad Conference*, pages 165–176.

Gu, Q., Tang, T., Cao, F., Song, Y.-d., and Member, S. (2014). Energy-Efficient Train Operation in Urban Rail. *IEEE Transactions on Intelligent Transportation Systems*, 15(3):1216–1233.

Haahr, J. T., Pisinger, D., and Sabbaghian, M. (2017). A dynamic programming approach for optimizing train speed profiles with speed restrictions and passage points. *Transportation Research Part B: Methodological*, 99:167–182.

Herr, N., Nicod, J.-m., Varnier, C., and Jardin, L. (2017). Decision process to manage useful life of multi-stacks fuel cell systems under service constraint. 105:590–600.

Hoffrichter, A., Hillmansen, S., and Roberts, C. (2016). Conceptual propulsion system design for a hydrogen-powered regional train. *IET Electrical Systems in Transportation*, 6(2):56–66.

Hong, Z., Li, Q., Han, Y., Shang, W., Zhu, Y., and Chen, W. (2018). An energy management strategy based on dynamic power factor for fuel cell/battery hybrid locomotive. *International Journal of Hydrogen Energy*, 43(6):3261–3272.

Hwang, H. S. (1998). Control strategy for optimal compromise between trip time and energy consumption in a high-speed railway. *IEEE Transactions on Systems, Man, and Cybernetics Part A:Systems and Humans.*, 28(6):791–802.

Iannuzzi, D. and Tricoli, P. (2012). Speed-based state-of-charge tracking control for metro trains with onboard supercapacitors. *IEEE Transactions on Power Electronics*, 27(4):2129–2140.

Jaafar, A., Akli, C. R., Sareni, B., Roboam, X., and Jeunesse, A. (2009). Sizing and energy management of a hybrid locomotive based on flywheel and accumulators. *IEEE Transactions on Vehicular Technology*, 58(8):3947–3958.

Jia, C., Qiao, W., and Qu, L. (2019). A cost-oriented control strategy for energy management of a dual-mode locomotive. In *2019 IEEE Vehicle Power and Propulsion Conference (VPPC)*, pages 1–6. IEEE.

Kampeerawat, W. and Koseki, T. (2019). Efficient urban railway design integrating train scheduling, wayside energy storage, and traction power management. *IEEJ Journal of Industry Applications*, 8(6):915–925.

Khayyam, S., Berr, N., Razik, L., Fleck, M., Ponci, F., and Monti, A. (2018). Railway System Energy Management Optimization Demonstrated at Offline and Online Case Studies. *IEEE Transactions on Intelligent Transportation Systems*, 19(11):3570–3583.

Khmelnitsky, E. (2000). On an optimal control problem of train operation. *IEEE Transactions on Automatic Control*, 45(7):1257–1266.

Lanneluc, C., Pouget, J., Poline, M., Chauvet, F., and Gerbaud, L. (2018). Optimal Energy Management of a Hybrid Train: Focus on Saving Braking Energy. *2017 IEEE Vehicle Power and Propulsion Conference, VPPC 2017 - Proceedings*, 2018-January:1–6.

Lhomme, W., Letrouve, T., Boulon, L., Jemei, S., Bouscayrol, A., Chauvet, F., and Tournez, F. (2018a). Ieee vts motor vehicles challenge 2019-energy management of a dual-mode locomotive. In *2018 IEEE Vehicle Power and Propulsion Conference (VPPC)*, pages 1–6. IEEE.

Lhomme, W., Sicard, P., and Bouscayrol, A. (2018b). Real-Time Backstepping Control for Fuel Cell Vehicle Using Supercapacitors. *IEEE Transactions on Vehicular Technology*, 67(1):306–314.

Li, Q., Wang, T., Dai, C., Chen, W., and Ma, L. (2017). Power management strategy based on

adaptive droop control for a fuel cell-battery-supercapacitor hybrid tramway. *IEEE Transactions on Vehicular Technology*, 67(7):5658–5670.

Liu, R. and Golovitcher, I. M. (2003). Energy-efficient operation of rail vehicles. *Transportation Research Part A: Policy and Practice*, 37(10):917–932.

Mendoza, D. S., Acevedo, P., Jaimes, J. S., and Solano, J. (2019). Energy management of a dual-mode locomotive based on the energy sources characteristics. In *2019 IEEE Vehicle Power and Propulsion Conference (VPPC)*, pages 1–4. IEEE.

Moskowitz, J.-P. and Cohuau, J.-L. (2010). Steem: Alstom and ratp experience of supercapacitors in tramway operation. In *2010 IEEE Vehicle Power and Propulsion Conference*, pages 1–5. IEEE.

Radu, P. V., Szelag, A., and Steczek, M. (2019). On-board energy storage devices with supercapacitors for metro trains-case study analysis of application effectiveness. *Energies*, 12(7).

Raghavendra Rao, A. and Mahesh, M. (2018). Analysis of the energy and safety critical traction parameters for elevators. *EPE Journal*, 28(4):169–181.

Rao, A. R., Mahesh, M., and Keshavan, B. (2018). Analysis of energy during regenerative modes. In *2018 IEEE International Conference on Power Electronics, Drives and Energy Systems (PEDES)*, pages 1–6. IEEE.

Saadat, M., Esfahanian, M., and Saket, M. H. (2016). Energy-efficient operation of diesel-electric locomotives using ahead path data. *Control Engineering Practice*, 46:85–93.

Sarma, U. and Ganguly, S. (2019). Design optimisation for component sizing using multi-objective particle swarm optimisation and control of pem fuel cell-battery hybrid energy system for locomotive application. *IET Electrical Systems in Transportation*.

Solano, J., Hissel, D., Pera, M.-C., and Amiet, M. (2011). Practical Control Structure and Energy Management of a Testbed Hybrid Electric Vehicle. *Vehicular Technology, IEEE Transactions on*, 60(9):4139–4152.

Solano, J., Mulot, J., Harel, F., Hissel, D., Péra, M. C., John, R. I., and Amiet, M. (2013). Experimental validation of a type-2 fuzzy logic controller for energy management in hybrid electrical vehicles. *Engineering Applications of Artificial Intelligence*, 26(7):1772–1779.

Sorrentino, M., Serge Agbli, K., Hissel, D., Chauvet, F., and Letrouve, T. (2020). Application of dynamic programming to optimal energy management of grid-independent hybrid railcars. *Proceedings of the Institution of Mechanical Engineers, Part F: Journal of Rail and Rapid Transit*, page 0954409720920080.

Steiner, M., Klohr, M., and Pagiela, S. (2007). Energy storage system with Ultracaps on board of railway vehicles. *2007 European Conference on Power Electronics and Applications, EPE*.

Strunz, K. and Brock, E. K. (2006). Stochastic energy source access management: infrastructure-integrative modular plant for sustainable hydrogen-electric co-generation. *International Journal of Hydrogen Energy*, 31(9):1129–1141.

Strunz, K. and Louie, H. (2009). Cache energy control for storage: Power system integration and

education based on analogies derived from computer engineering. *IEEE Transactions on Power Systems*, 24(1):12–19.

Taguchi, G. and Phadke, M. S. (1989). Quality engineering through design optimization. In *Quality Control, Robust Design, and the Taguchi Method*, pages 77–96. Springer.

Wagner, J. R., Mount, E. M., and Giles, H. F. (2014). Design of experiments. In Wagner, J. R., Mount, E. M., and Giles, H. F., editors, *Extrusion (Second Edition)*, Plastics Design Library, pages 291 – 308. William Andrew Publishing, Oxford, second edition edition.

Yang, Z., Yang, Z., Xia, H., and Lin, F. (2018). Brake Voltage Following Control of Supercapacitor-Based Energy Storage Systems in Metro Considering Train Operation State. *IEEE Transactions on Industrial Electronics*, 65(8):6751–6761.

Yedavalli, K., Guo, L., and Zinger, D. S. (2011). Simple control system for a switcher locomotive hybrid fuel cell power system. *IEEE Transactions on Industry Applications*, 47(6):2384–2390.

Yin, J., Tang, T., Yang, L., Gao, Z., and Ran, B. (2016). Energy-efficient metro train rescheduling with uncertain time-variant passenger demands: An approximate dynamic programming approach. *Transportation Research Part B: Methodological*, 91:178–210.

Yoneyama, T., Yamamoto, T., Kondo, K., Furuya, T., and Ogawa, K. (2007). Fuel cell powered railway vehicle and experimental test results. In *2007 european conference on power electronics and applications*, pages 1–10. IEEE.

Appendix

Appendix A. Results for the speed profiles used in the parameters identification

This annex presents the power distribution between the system sources, the states of charge of the energy storage elements and the voltage on the DC bus, for 3 different speed profiles provided by the organizers of the IEEE VTS Motor Vehicles Challenge. These results were obtained using the same EMS. The EMS used is the presented one in the Chapter 3.1 and its parameters were tuned using the methodology presented in the Chapter 4.

Each profile is characterized by its maximum speed. The maximum speeds are 50km/h, 100km/h, 140km/h and the speed profiles are called respectively P50, P100 and P140.

Speed profiles provided the organizers of the IEEE VTS Motor Vehicles Challenge

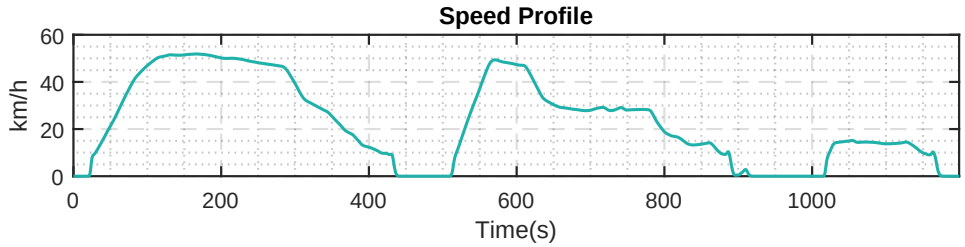

Figure 17. Traction + auxiliaries power and Speed profile - P50

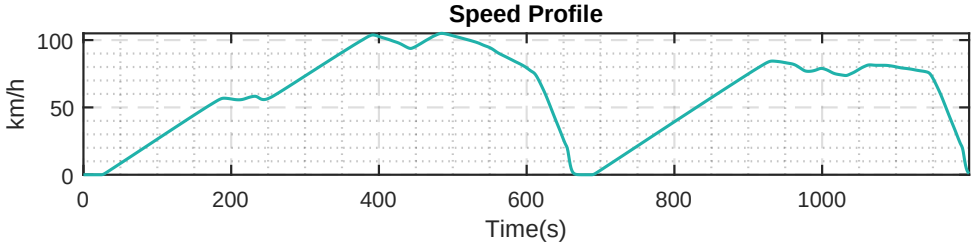

Figure 18. Traction + auxiliaries power and Speed profile P100

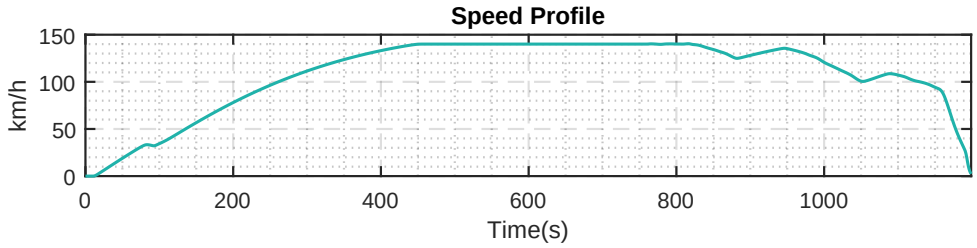

Figure 19. Traction + auxiliaries power and Speed profile P140

Appendix B. Locomotive Characteristics

This appendix presents the locomotive characteristic such as their physical, electrical and mechanical components. The Table 3 presents the general locomotive parameters, Table 5, Table 6 and Table 7 present the parameters for the Fuel Cell system, battery system and supercapacitor system respectively. The Table 4 presents the objetive function elements related to the cos per unit of primary energy. . All this information is provided by the IEEE Motor Vehicles Challenge Organizators Lhomme et al. (2018a)

Table 3
Main parameters of the studied locomotive

Locomotive	
Mass	140t
Maximal speed	140km/h
Number of traction drive	4
DC **bus**	
Voltage range of the DC bus	$1000-1900$V
Capacity of the DC bus	40mF
DC **overhead line**	
Voltage of the catenary	1500V
Resistance per unit of length	0.1Ω/km

Figure 20. New EMS - P50

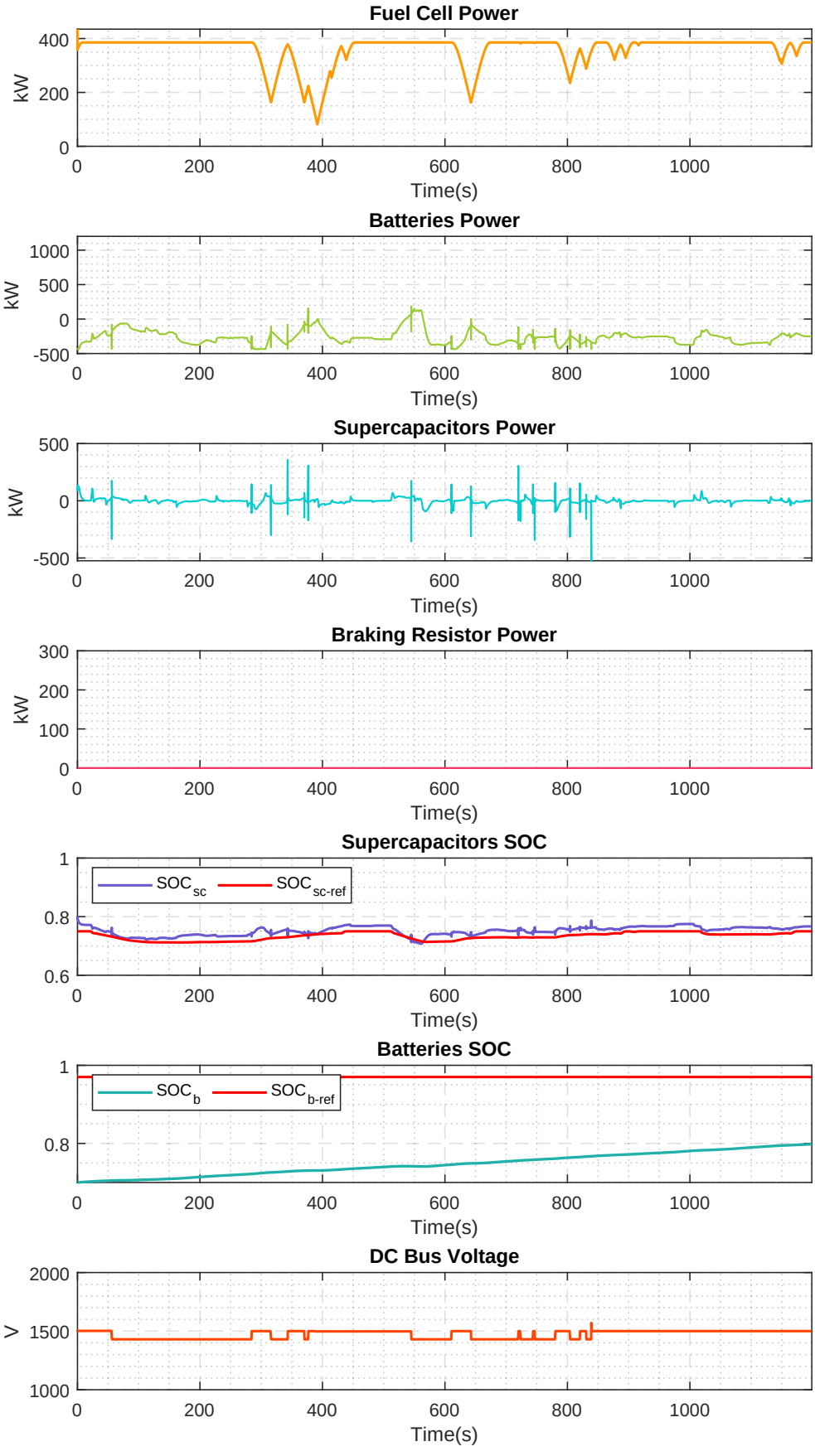

Table 4
Cost calculation

Cost calculation	
cost of the electricity network per unit of energy	70€MWh
cost of the hydrogen per unit of hydrogen mass	3€kg
cost of the fuel cell per unit of power	40€/kW
cost of the supercapacitors per unit of Farad	8€∈ /F
cost of the supercapacitors per unit of energy	7900€/kWh
cost of the battery per unit of energy	200€/kWh

Table 5
Fuel Cell Characteristics

Fuel Cell	
Type of fuel cell	PEMFC
Number of cells in series	350
Number of modules in parallel	2
Voltage range of a cell	$0.3-0.75$V
Active surface of a cell	950cm^2
Maximal variation rate of the current	50A/s
Maximal current of a cell	1400A
Minimal current of a cell	0A
Rated power of a cell	570W
Rated power of the fuel cell system	399kW
Efficiency range of the chopper	$90\,\%-96.5\,\%$
Maximal power of the chopper	500kW

Table 6
Battery Characteristics

Battery	
Type of battery	LiFePO4
Number of cells in series	158
Number of branches in parallel	10
Total number of cells	1580
Rated capacity of a cell	160Ah
Rated voltage of a cell	3.8V
Maximal voltage of a cell (charge)	4.0V
Minimal voltage of a cell (discharge)	2.8V
Maximal current of a cell	$2\text{C} = 320\text{A}$
Minimal current of a cell	$-0.5\text{C} = -80\text{A}$
Minimal state of charge	20 %
Initial state of charge	70 %
Rated energy of the battery	935kWh
Usable energy of the battery	748kWh
Efficiency range of the chopper	$95\,\% - 98.8\,\%$
Maximal power of the chopper	2MW

Table 7
Supercapacitors Characteristics

Supercapacitors	
Type of electrolyte	Organic
Number of SC in series	280
Number of branches in parallel	5
Total number of cells	1400
Rated capacity of a cell	5000F
Rated voltage of a cell	2.7V
Maximal current of a cell	1900A
Minimal current of a cell	−1900A
Minimal state of charge	35 %
Initial state of charge	80 %
Rated energy of the supercapacitors	7.09kWh
Usable energy of the supercapacitors	4.61kWh
Efficiency range of the chopper	85 % − 94.3 %
Maximal power of the chopper	2MW

Figure 21. New EMS - P100

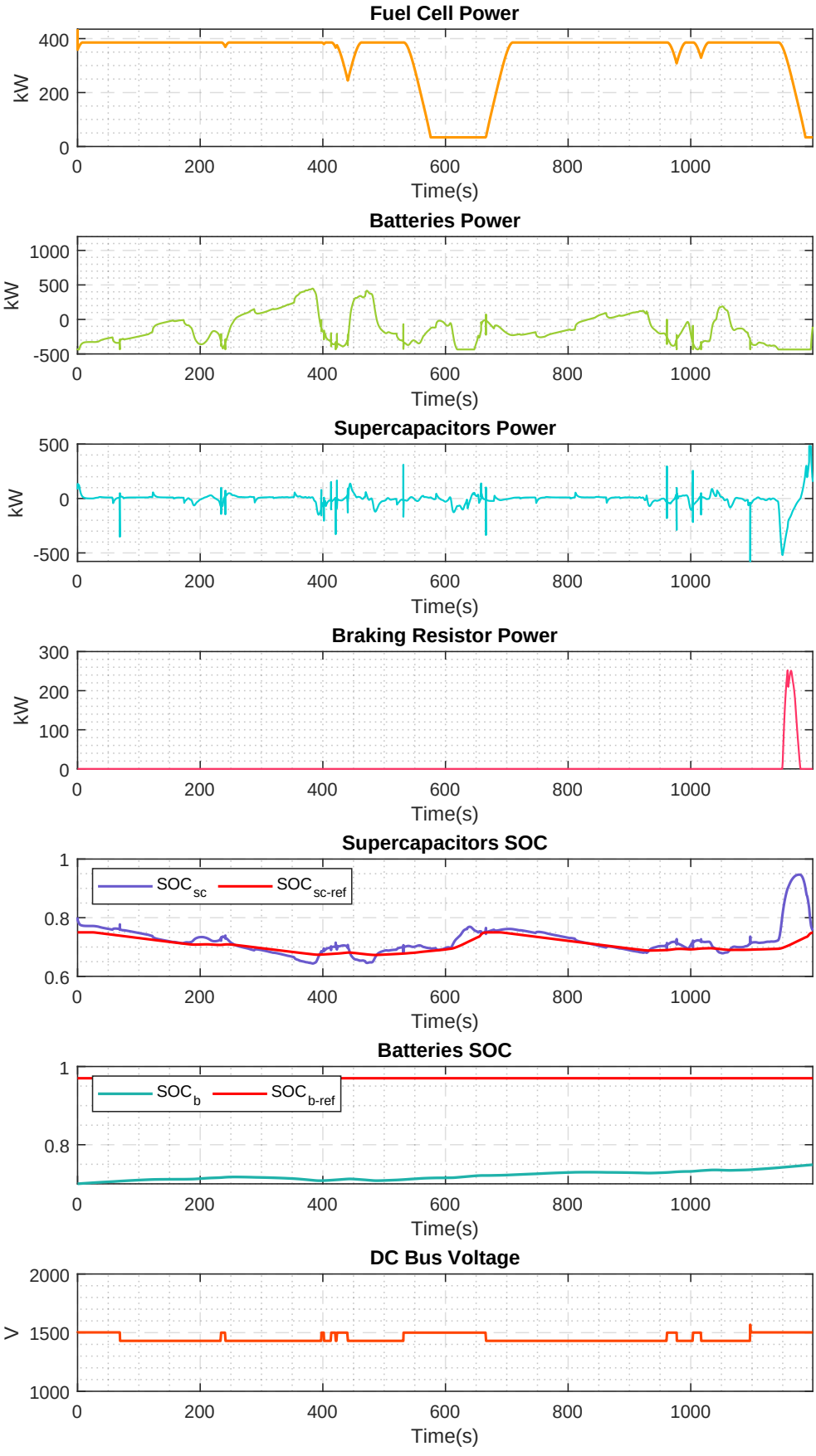

Figure 22. New EMS - P140

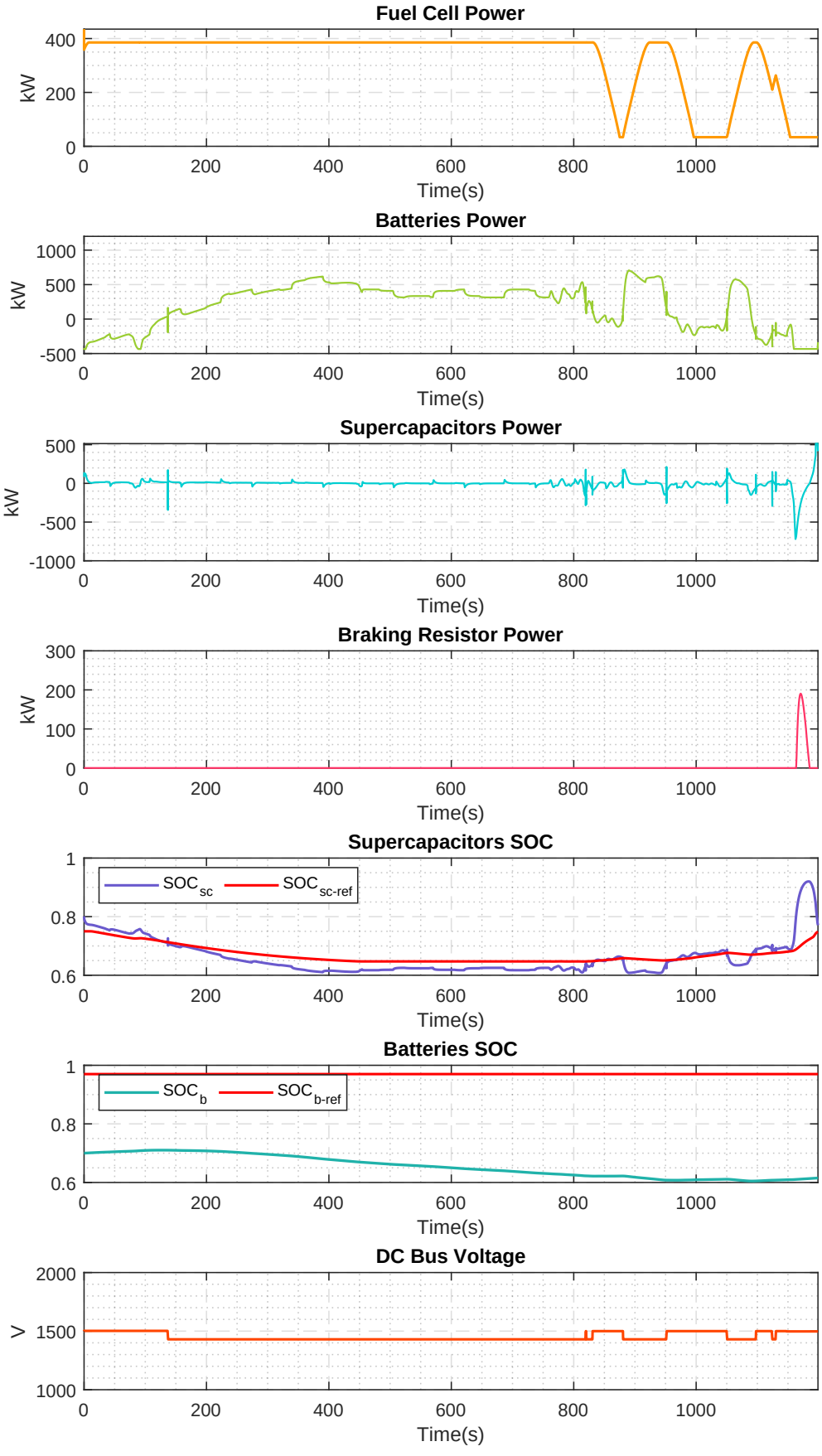

Figure 23. Results speed profiles with second H_2 consumption model - P50

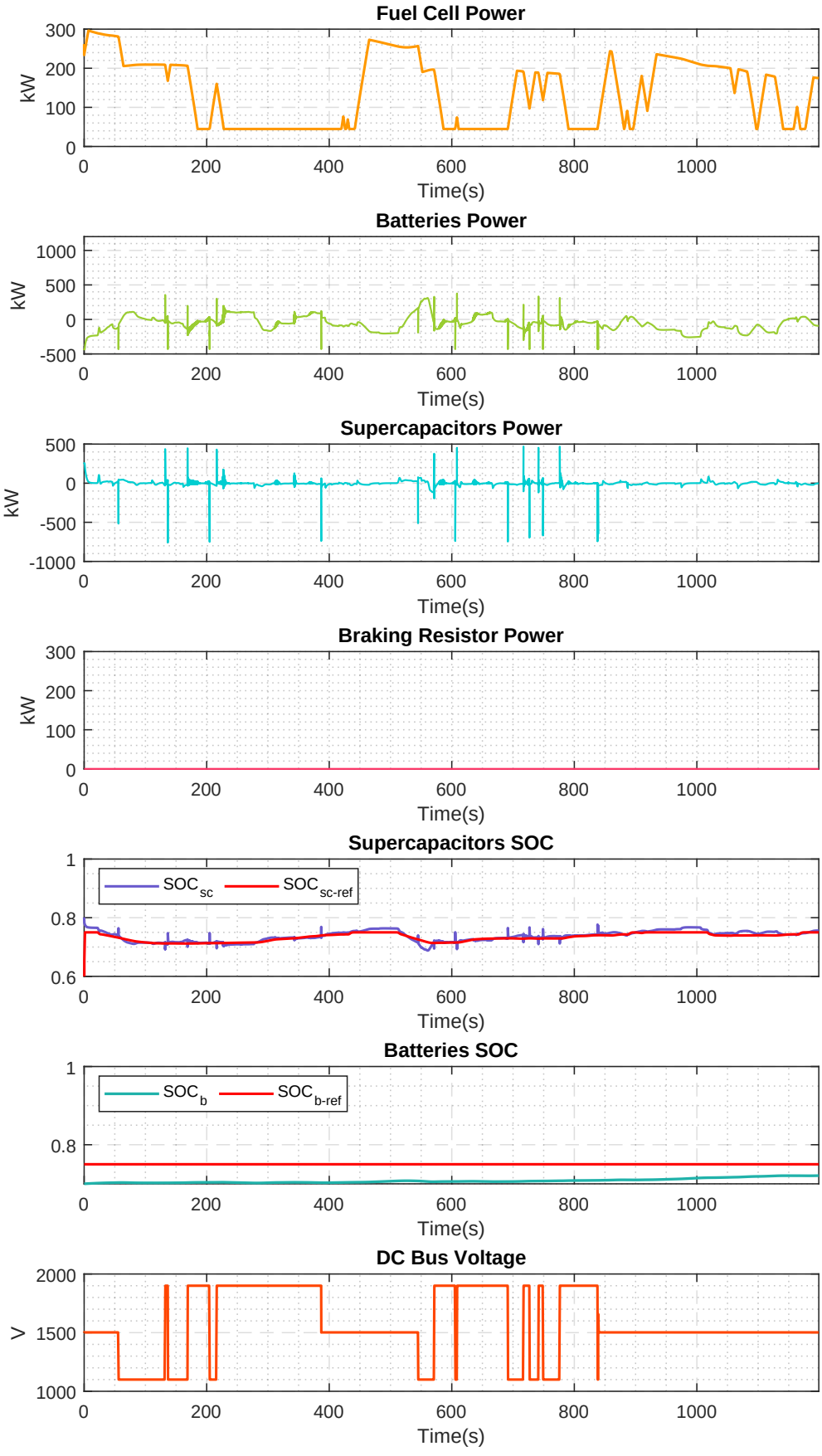

Figure 24. Results speed profiles with second H_2 consumption model - P100

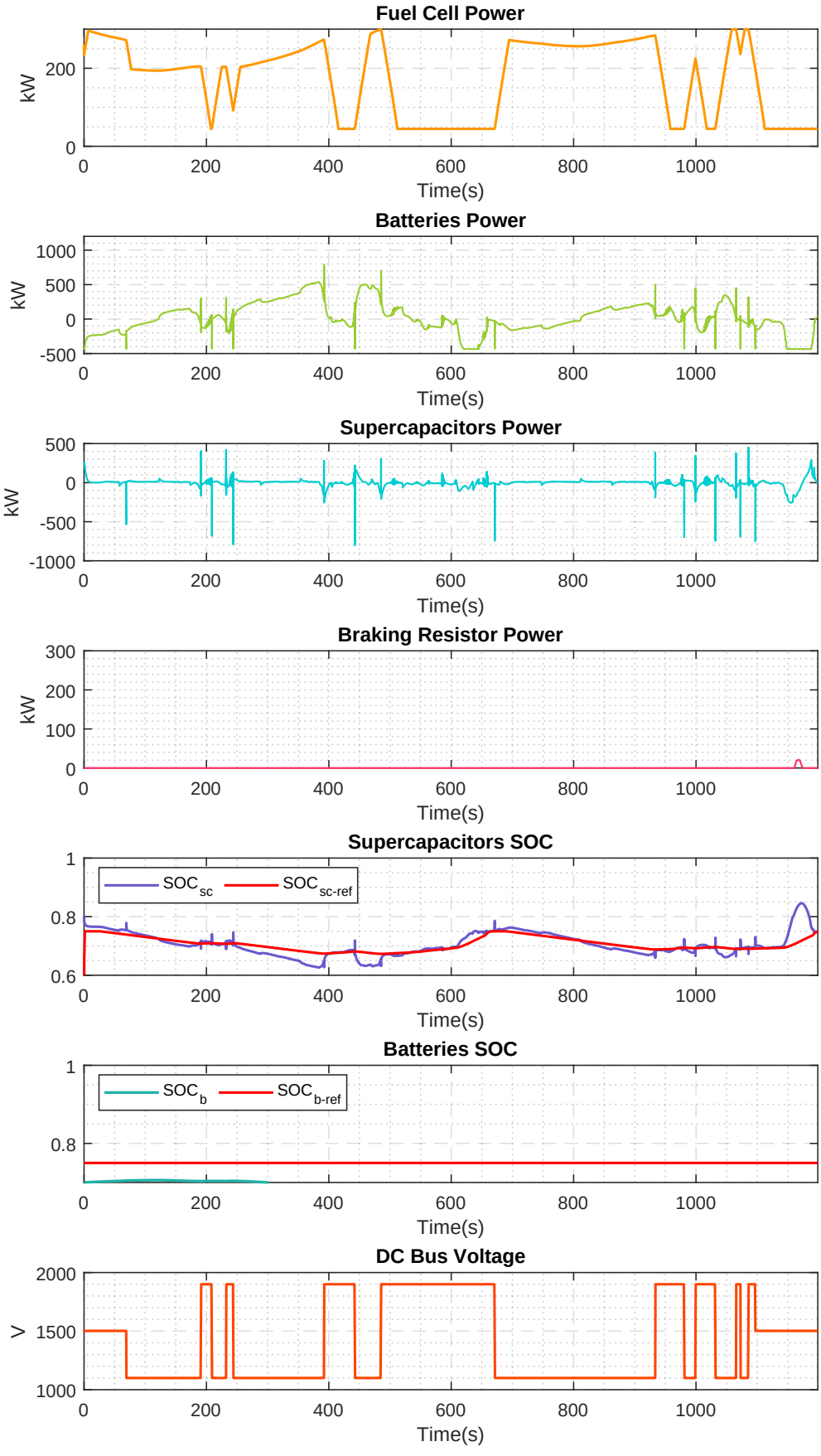

Figure 25. Results speed profiles with second H_2 consumption model - P140